A NUMERICAL STUDY ON THE EFFECT OF BOW FLARE ANGLE ON GREEN WATER LOADING ON FPSO

By

SUNKYU LEE

Submitted for the Degree of Master of Philosophy

Department of Naval Architecture, Ocean and Marine Engineering

University of Strathclyde

May 2018

Declaration of Authenticity and Author's Rights

This thesis is the result of the author's original research. It has been composed by the author and has not been previously submitted for examination which has led to the award of a degree.

Signed:

Date:

Acknowledgements

Firstly, I would like to thank my supervisor Dr. Yigit Demirel of the Department of Naval Architecture, Ocean and Marine Engineering at the University of Strathclyde. He has consistently helped me to move in the right direction for my research and has helped me to study in the best possible environment. Also, there was no major difficulty in studying by giving feedback continuously while meeting regularly.

Secondly, I also would like to thank the professor Young-gil Lee of the Department of Naval Architecture and Ocean Engineering at the University of In-ha in Korea. He gave me an opportunity to study at the University of Strathclyde. And he continued to help me a lot while I was studying in here.

Finally, I used HPC computer when I calculated my simulations. So results were obtained by using the EPSRC funded ARCHIE-West High Performance Computer (http://www.archie-west.ac.uk), EPSRC Grant No. EP/K000586/1.

Thanks to everyone

Sunkyu Lee

Abstract

When there are the strong waves, green water phenomenon has a number of negative effects on ship or floating structures such as damaging structures on the deck and degrading the stability of the ship. Floating production storage and offloading vessels (FPSO) are commonly operated at a certain position and located to encounter mainly bow waves for the purpose of a decrease in roll motions.

This study is focused on the analysis of the effects of the bow flare angle above the free surface on the hydrodynamic loads associated with the green water phenomenon.

When designing the bow flare angle of the FPSO considering the influence of the green water, it is very important to understand the amount of the green water and the impact load on the superstructure on the deck. These are the functions of the bow flare angle of the FPSO as well as the freeboard exceedance level.

Firstly, this study discusses the water level on the deck. Then the flow velocities on the deck are presented. And the pressure on the deck is also considered. Finally, a method of determining green water impacts on structures on the deck is presented. For these four sections, the relation with the wave height and wave period level are given.

Key words: Green water, FPSO, bow flare angle, wave height, wave period, wave velocity

Contents

List of Figures

1 Introduction

1.1 Green water

In rough seas, the waves and ship motions become larger that results in water ingress on the deck of a ship. This phenomenon is widely called ‘Green water loads’. The term of green water is used to distinguish the spray phenomena around the ship from the actual solid seawater on the deck. Because the seawater is green, not blue, the term green water is commonly used.

In recent years, ship type offshore units are often used to produce and store oil at the same time in spite of severe sea environment. The Floating Production Storage and Offloading units (FPSO) that remain long at a certain location in the oceans should not be severely damaged under extreme environmental conditions.

This need a proper mooring system, but also to pay attention to the problem of the green water on the deck. When there is plenty of space on the deck of the tanker, the FPSO deck is loaded with a lot of sensitive equipment. Because the FPSO is commonly connected to the mooring system using a rotating turret, so important equipment is near the bow. Furthermore, the rotating turret results in a weather-vaning character of the vessel, exposing the bow to the most critical wave conditions. Therefore, the green water can adversely affect such equipment such as the fluid swivels, piping, turret structure, control valves, emergency systems, fire detection and protection systems and cable trays. For FPSO units with the superstructure on the bow, the same applies to the front of the superstructure.

Events in the North Sea and Norway have confirmed that FPSOs are exposed to the green water phenomenon. Morris, Millar and Buchner (2000) reported that 17 large and small green water accidents were identified in 12 UK FPSOs and FSUs (Floating Storage Units) since 1995. Some FPSOs and FSUs have experienced more than one accident.

1.2 Problem definition of this study

Green water problem is very complex and non-linear. It is a result of a very large number of parameters (freeboard, underwater hull shape, above water hull shape, draft, deck shape, loading conditions, ship speed, wave height, wave period, wave heading and so on). This is confirmed by the work presented by Watanabe, Ueno and Sawada (1989) and Watanabe (1990) on the effect of bow flare shape of a container ship. They also point to the complex deformation of the incoming wave profile by the bow flare angle. A study of Takagi and Naito (1993) presents interesting observations on the effect of the hull shape on the final flow pattern on the deck.

Due to this complexity, a bow shape that is very effective to keep the deck dry in the condition can be less ideal in other environmental conditions.

From the green water problem, it can be concluded that green water is a critical issue for ship-type offshore structures.

Also, the solution is very limited because it is a very complicated and nonlinear green water problem, to solve these problems, it is necessary by assuming a wide range using prediction methods. To solve these problems, further studies of green water propagation on the deck in detail are needed.

Ship-type offshore structures, however, have much more sensitive equipment on their decks than merchant vessels and even naval vessels. This requires detailed insight in the flow on the deck and the resulting green water loading.

Researchers on the green water phenomenon have already done a lot of research. For example, the probability of green water occurrence, the water level on the deck, the flow pattern on the deck, hydrodynamic loads on the deck by green water, and so on. The research on the possibility of the green water occurrence has been investigated by many researchers, and we have successfully studied many cases by combining the linear potential flow theory and the probability theory (Soares and Pascoal, 2005).

1.3 Historical overview of green water research

Green water problem has been the subject of study and debate since the early days of research into ship behaviour at the end of the Nineteenth Century. One of the first to research green water on FPSOs is Buchner (1995).

By comparing model tests with response calculated with linear diffraction theory, several observations were made. Large relative wave motions generally occur when the wave frequency is just above the peak frequency in the pitch response. It is also observed via model tests that the use of linear diffraction theory for the green water problem at the bow is limited.

The probability of green water at the bow of a FPSO is studied in 1998 by Hamoudi and Varyani (1998). It was found that the probability of deck wetness depends mainly on the relative wave motions but also on, for example, environmental conditions. For the probability of green water, the formula given by Price and Bishop (Price and Bishop, 1974) was used, which depends on the various of the relative bow motion. The relative bow motion was measured and applied to predict the probability of deck wetness. It was found that the probability increases as the significant wave height increase. The wave period does not affect the probability. Increasing the freeboard height decrease the probability. The wave velocity does not relate to the velocity of the water on the deck because the bow heavily disturbs the flow.

Faltinsen et al. (2002) developed a two-dimensional method that satisfies the non-linear free surface conditions of the potential theory exactly. The method is partly validated by model tests. A trim angle of up to 5degrees was found not to affect the green water problem.

A new method for measuring the water velocity of green water to develop a green water velocity profile was tested by Ryu at el. (2007). The wave run-up on a fixed model was measured. For the wave run-up a maximum velocity of 2.9 times the phase velocity of the incoming wave was found. For the maximum horizontal velocity during the entire green water event, this was 1.13 times the phase velocity of the incoming wave. The maximum vertical velocity occurred before the water moved on the deck. The dominant velocity before the wave hits the model is horizontal, directly in front

of the model, though when the wave hits the model, the dominant velocity is vertical and the dominant velocity of the water on deck is horizontal again.

Considering the influence of the green water, many factors must be considered when designing FPSO. Here are three factors: (a) FPSOs are installed by a mooring system and is located at a specific location for a long period of time; (b) FPSOs is positioned such that the waves run directly against the bow of the ship, in order to reduce the roll motion; and (c) FPSOs need to operate without being damaged even in extreme sea conditions and deep water. These factors can make the bow region of FPSO more susceptible to green water loads. Therefore, the bow shape of FPSO should be appropriately designed to reduce the effects of green water. In fact, there have been reports of FPSO green water accidents causing serious damage to the structures on the deck and causing operational problems (Ersdal and Kvitrud, 2000).

1.4 Main aims and objectives

The main aim of this thesis is to investigate the effects of the bow flare angle above the free surface on the hydrodynamic loads associated with the green water phenomenon. Specific objectives are listed below, with each detailing the novelty of each chapter:

- To validate the pressure value of EFD results which was performed in Seoul National University (Hyun-ho et al., 2012).

- To design and compare the ships which have different bow flare angle.

- To develop and propose a CFD model which enables the prediction of the effect of the bow flare angle.

- To predict the effects of bow flare angle when the green water phenomenon occurs.

- To investigate and show the applicability of a CFD method for the simulation of green water phenomenon.

- To consider the water level on the deck when the bow flare angle is changed.

- To consider the pressure on the deck when the bow flare angle is changed.

- To analyse the relation between the green water on the deck and the impact load on the superstructure.

1.5 Structure of this thesis

The structure of this thesis is summarised below:

- Chapter 2 presents literature review from a critical point of view and present brief theoretical information about the subject

- Chapter 3 presents the general methodology followed in this thesis.

- Chapter 4 describes the ship used in the study and describe how bow flare angle was designed. It also describes the wave conditions used in simulations.

- Chapter 5 proposes a computational fluid dynamics (CFD) model which enables the prediction of the effect of bow flare angle when the green water phenomenon occurs.

- Chapter 6 presents the validity of the model is demonstrated by comparing the results with the experimental data. And this chapter describes the simulation results accomplished in this study and it is divided into five sub-section, each of which presents different aspects of findings.

- Chapter 7 presents a discussion on the outcome of this thesis and the concluding marks. It also outlines some recommendations for future works of research.

2 Literature review

2.1 Ship motions and relative wave motions

When the green water occurs, ship motions and relative motions around the bow play an important role. As observed in the previous section, the relative wave motion around the bow is one of the various factors that cause the green water phenomenon. The relative wave motion is defined as the difference between the heave motion of the ship and the wave height of its motions right in front of the bow. As soon as the relative wave motions exceed the freeboard level, the green water phenomenon occurs as the water penetrates onto the deck. The relative wave motions should, therefore, be predicted accurately to come to a reliable prediction of green water loading. The relative wave motions are a function of both the ship motions and wave motions, with all their non-linearity.

And two dimensional linear (or non-linear) strip theories are the basis for mostly green water prediction methods for slender naval and merchant vessels. However, for full ship-type offshore structures when predicting relative motions and motions three dimensional linear diffraction analysis is mainly used, see for instance Van Oortmerssen (1973). In linear diffraction analysis the wave exciting forces on the ship due to the undisturbed waves and waves reflected on the hull are determined. In addition, when using this method, the added mass and the damping due to the wave generated by the ship motion are also calculated.

In linear analysis, any exceeding of the freeboard height by the relative wave height will lead to an equivalent amount of water on deck. This estimation is the basis of the green water prediction methods by Ochi (1964) and Fukuda, et al. (1973). However, as shown experimentally by both Buchner (1995) and Ogawa, et al (1998), exceeding the freeboard do not necessarily lead to an identical water height on deck.

2.2 Water flow onto deck

As was reported by Goda, Miyamoto and Yamamoto (1976) and Vermeer (1980), there is a clear resemblance between most cases of green water flow on the deck and the theoretical dam breaking problem. In this theoretical problem, described extensively by Stoker (1957), it is assumed that at time t=0 there is a vertical wall of water of height on one side of a vertical dam. At that moment the dam is removed and the water flows into the empty region. The flow velocity into the empty region is proportional to the square root of the height of the water before the dam breaks.

Goda, Miyamoto and Yamamoto (1976), Vermeer (1980), Dillingham (1981) and Mizoguchi (1998) applied the theoretical results of the dam breaking problem to the calculation of the flow of the water onto the deck.

Although the theoretical dam breaking does show clear resemblance with the typical green water flow onto the deck, it will be clear from a comparison between the theoretical dam breaking and the typical green water flow onto the deck that the actual flow is far more complex.

- The ship deck is moving.
- The height of the freeboard exceedance is varying in time.
- The initial velocity is not per definition zero and is influenced by wave kinematics and run up effects. This is especially of importance when steep and energetic waves reach the deck, as reported by Hellan, Hermunstad and Stansberg (2001).

Despite these things, the dam breaking model can help to understand the green water physics better.

2.3 Effect of flare angle of ship

The presence of bow flare angle of the ship affects both the relative motion and the diffraction of the incoming wave. This influences the resulting water level on the deck

and the dynamics of the green water on the deck. Most methods for determining the relative motions are based on linear diffraction analysis, where exciting forces on the ship due to the waves and the reflected waves are determined. This method only takes into account the ship's geometry up to the still water line, and the geometry below the still water line is not included. It also neglects the effect of dynamic swell, which is the increase of the water level near the ship as a result of the presence of the hull in the wave. Buchner (1995) and Buchner (1996) also showed experimentally that for a moored FPSO, a change in the bow geometry when more flare is added to the bow above the still water line may increase the relative motion.

Regarding the resulting water height on deck, Buchner and Voogt (2000) showed, also for a moored FPSO, that an approximate linear relation exists between the relative exceeding of the freeboard and the resulting water level on deck and that the factor between them depends on the flare of the ship's bow. The experiments clearly showed that the actual water level on the deck, resulting from the relative exceeding of the freeboard, is significantly reduced with increasing bow flare.

In a previous work O'Dea and Walden (1984) investigated the effect of flare on green water loads, by applying significant flare to traditional ship types, and the conclusion was that the deck wetness was reduced as a result of the increased flare. In another study by Lloyd, et al. (1985), the effect of flare was also investigated by applying different bow configurations to a frigate type ship, and they concluded that a heavily flared bow increases the deck wetness. Though these two conclusions contradict each other, they may still both be true. Since it is known that flaring of the bow will alter the response of the ship for a given wave, this can in some cases where the ship motion at the bow comes out of phase with the relative motion, decrease the relative motion and thus reduce the amount of shipped water, whereas in other cases, the increased relative motion will increase the relative wave at the bow and thus increase the amount of shipped water.

To illustrate the disagreement in the maritime community regarding the effect of bow flare on deck wetness Lloyd et al. (1985) give a list of previous works, and it is clear that there are many different opinions on this topic, which illustrates the complexity.

2.4 Water behaviour and loading on deck

The velocities and pattern of the water on the deck, also the pressure on the deck of the vessel is of importance for the design. In the earlier study of Buchner (2002) on the prediction of the pressure for frigates with forward speed, investigations showed that the large pressure peaks occurred at some point that the water level on the deck at a certain position increased rapidly. This indicated that the rate of change of water level on the deck has an important effect on the maximum deck pressures

However, for a ship-type offshore structure the accelerations are generally at their maximum at that moment the water comes onto the deck. Consequently, the vertical velocity is close to zero. This results in a pressure at the deck that is dominated by the static pressure and the acceleration component.

On the other hand, it should be noted that the largest water level on the deck occurs in front of structures, such as deckhouses. At that moment that the fluid flow is blocked by a structure, the water is running up in front of it. This can have a large effect on the maximum water pressure on the deck. Another important type of impact loads can come from water running up in front of a structure such as the hatches of a ship and falling back on its top,

2.5 Green water impact on structures

When the green water occurs, and there is a high water level and a high velocity flow on the deck of the bow region, there can be a tremendous impact on the superstructure on the deck. After some point, when the water on the deck hits the superstructure, a huge height of water column is formed. After that, the water column collapses and puts large pressure on the deck.

In can be divided into three stages from the incident waves strike the bow until reach the superstructure as follows:

1) In a step called impact stage, the first maximum pressure is generated on the deck. At this time, it is called the rising time from the incident wave hit the bow of the ship until the maximum pressure value is generated on the deck.
2) In a step called quasi static load stage, most of the kinetic energy of the fluid disappears, and water strikes the superstructure, and then it forms a large water column in front of the superstructure.
3) In a step called plunging water stage, as the high water column created in the previous step collapses, a large pressure is generated to the deck, where the secondary maximum pressure occurs.

Sometimes minor peak loads are observed in the early stages of the impact. These are a result of fast thin water jets in front of the main amount of green water. However, the impulse of these initial load peaks is small.

The process for the green water phenomenon depicted above is very similar to a jet impinging perpendicularly at the plate. Based on experiments with such a set-up, Suhara, Hiyama and Koga (1973) found that the pressure peak is dependent on the square of the velocity.

3 Methodology

This section will outline the methodology of this thesis. It will play a good role in briefing the overall content of the thesis. Figure 1 below depicts the overall methodology in this thesis.

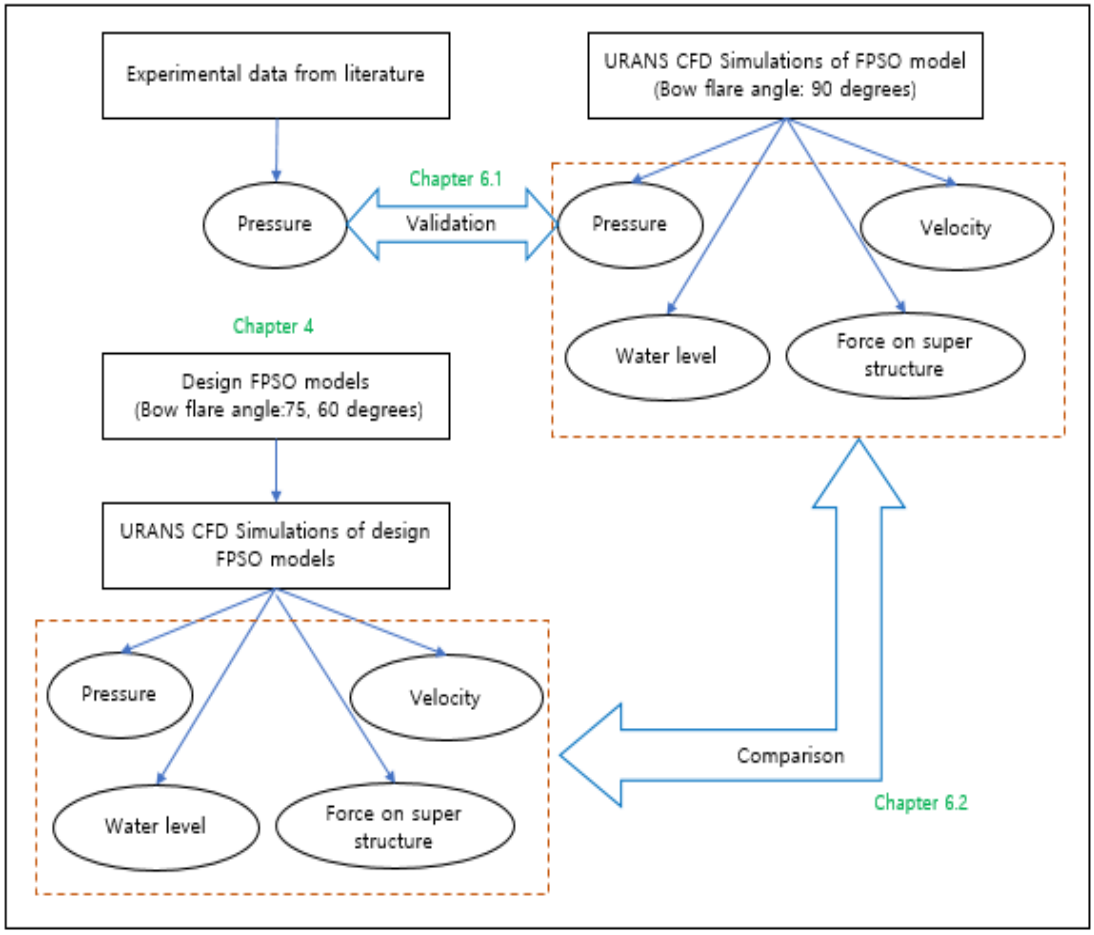

Figure 1 The methodology in this thesis.

First of all, in chapter 3, after defining the bow flare angle, the design FPSO models which have bow flare angles of 75 and 60 degrees will be explained how to change bow flare angle.

Secondly, in chapter 4, details of the numerical simulation approaches used in this thesis will be provided and the numerical methods applied to the CFD model which

enables the prediction of the effect of the green water phenomenon such as pressure, water level on the deck, water velocity above deck will be discussed.

Then, in order to validate, EFD data obtained from the experiment of Hyun-ho Lee (2012) was used. In EFD, five piezo-resistive type pressure transducers were used for pressure measurements at selected locations on the deck. The locations of pressure measurements were the same for all FPSO models. The analogue signals procured from the sensors were converted into digital signals via an A/D converter (Hyun-ho Lee, 2012).

Afterwards, weighted arithmetic mean will be used to analyse overall trends of the pressure and water level on the deck when the green water occurs. The pressure applied at each position was calculated as a ratio to the overall pressure of the deck, and the ratio was set as a weighted coefficient at each position, so that the overall pressure applied to the deck was compared with other design hulls. The weighted arithmetic mean is similar to the most common arithmetic mean used, however, instead of each data point contributing equally to the final average, some data points contribute more than other data points. A description of the weighted arithmetic mean is given in chapter 5.6.

Then, the developed and proposed CFD approach is used, the CFD commercial program Star-CCM+ was used to calculate the FPSO model to obtain the CFD results. And then a comparison of EFD and CFD results of pressure on the deck is given in chapter 6.1. As discussed by the International Towing Tank Conference (ITTC), advances in numerical modelling methods and increases in computational power have made it possible to carry out fully non-linear simulations of ship motions, taking into account viscous effects, using CFD. In this study, an unsteady RANS approach is applied using the commercial CFD software Star-CCM+ version 11.04, which was developed by CD-Adapco. Additionally, the supercomputer facilities at the University of Strathclyde have been utilised to allow much faster and more complex simulations. As computational facilities become more useful and accessible, using three dimensional techniques to study green water problems is becoming more common. As explained in detail by Tezdogan et al. (2014a), Yasukawa (2003) claims that three dimensional methods have been developed to overcome the shortcomings in the strip

theory methods. In the method developed by Bertram and Yasukawa (1996), full three dimensional effects of the flow and forward speed are accounted for, in contrast to strip theory where these effects are not properly taken into account. Yasukawa (2003) applied the theory of Bertram and Yasukawa (1996) to several container carriers with strong flare. As a result of his study, it was reported that hydrodynamic forces, ship motions and local pressures are much better predicted suing the theory of Bertram and Yasukawa (1996) than the results obtained by strip theory when compared to experiments. However, the predicted lateral hydrodynamic forces are not satisfactory, due to the viscous flow effect. Yasukawa (2003) suggests that this problem can be diminished by applying empirical corrections, similar to those employed in strip theory. Simonsen et al. (2013) highlight that the effects which are ignored in the potential theory such as breaking waves, turbulence and viscosity should be directly taken into account in the numerical methods. RANS methods, for example, are better alternatives to the potential flow theory as they can directly incorporate viscous effects in their equations. Due to these reasons, a decision was therefore made to use the FPSO model in the CFD simulations presented in this paper

Finally, after validating CFD results with EFD results, the results of the water level, pressure on the deck, water velocity above the deck and force on superstructure will be compared to see the effect of the bow flare angle when the green water occurs in chapter 6.2. In order to compare the pressure and water level on the deck according to the bow flare angle, a time series graph in one period will compared.

4 Ship geometry and wave conditions

4.1 Ship geometry

The main dimensions of the FPSO prototype are as follows. Its length is 300m, it has a width of 60m and a depth of 30m. This is similar to the dimensions of a typical large FPSO and was reported by Wang and Spong (2003). And the freeboard is an important in the green water phenomenon, which was set at 1.5% of the length of the ship. The freeboard (f), a very important factor in the green water phenomenon, was set at 1.5% of the length of the ship, that is, 4.5m considering full load condition (Barcellona et al., 2003).

Model tests which is experimented in Seoul university were done in the towing tank, which measures 100 m long, 8 m wide, and 3.5 m deep and is equipped with a flap type wave-maker (Hyun-Ho et al., 2012). The length of the FPSO model in this study was set at 3m, which is the 1/100 scale ratio of the prototype FPSO. In order to focus on the deck pressure, water level on the deck and flow propagation process by only the green water, in this study the ship motions did not considered. All the results were obtained using a fixed model and these results cannot be correlated with results from free motions. Using of the fixed model does not affect the results even with the truncated model, so the model is used at 1.5m length, which is half of the total length of the ship. Fig. 2 shows geometry of the FPSO model which has 90 degrees bow flare angle.

	Ship	Model
Scale ratio	1	1/100
L_{BP}	300m	3.00m
Breadth	46.00m	0.307m
Depth	26.60m	0.177m
Freeboard	8.25m	0.055m

Table 1 Principal dimension of the FPSO model *(Hyun-Ho et al., 2012).*

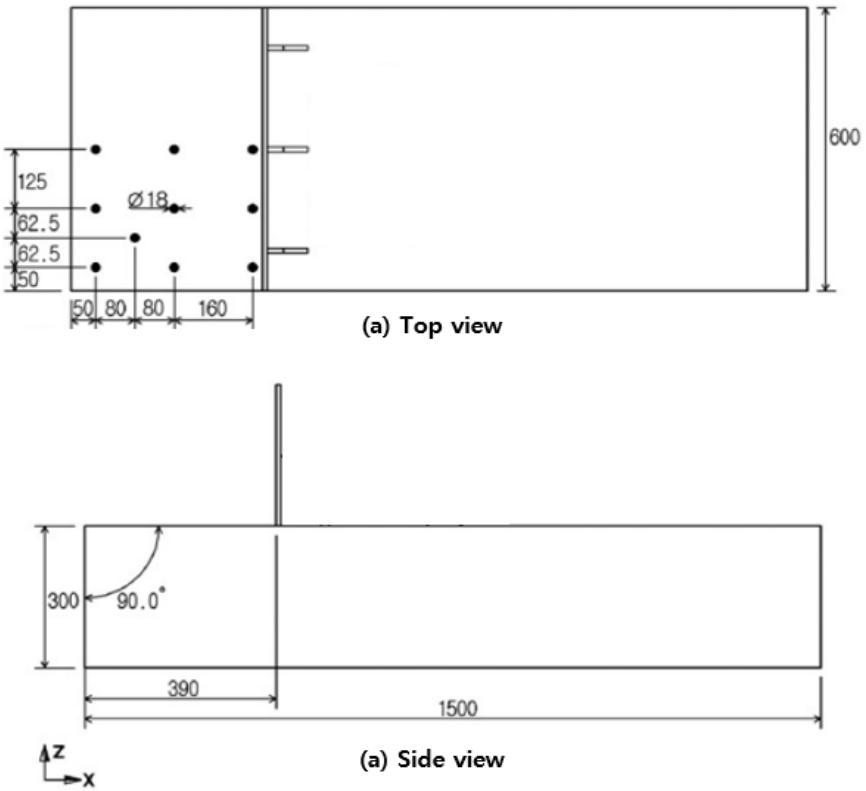

Figure 2 Geometry of the FPSO model which has 90 degrees bow flare angle *(Hyun-Ho et al., 2012).*

The purpose of this study to investigate the green water and the impact load on the deck of ship which has various bow flare angles. Barcellona, et al. (2003) has been researched about effect of deck shape. Their studies have shown that the deck shape effects the flow pattern on the deck and impact load of green water as well.

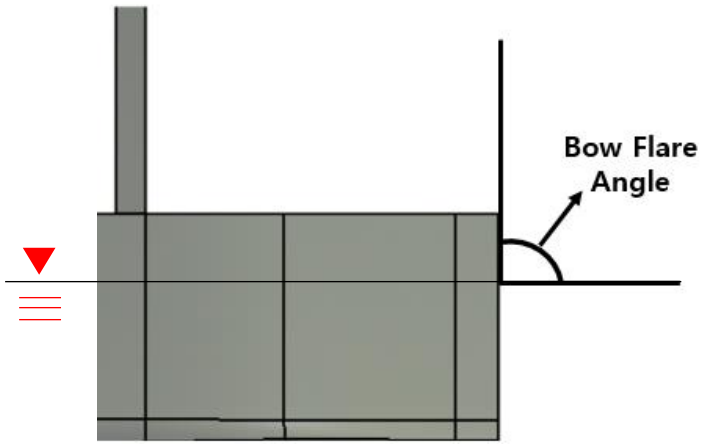

Figure 3 Definition of bow flare angle.

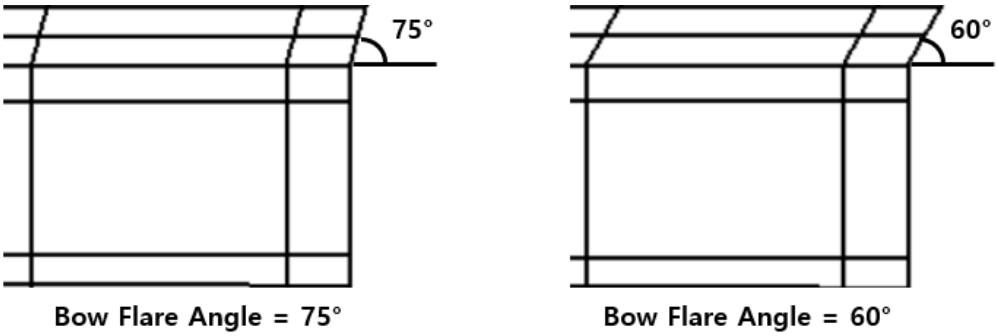

Figure 4 Two different FPSO bow models.

Fig. 3 shows the definition of the bow flare angle. The flare angle is defined as the angle between the still water line and the line from the still water line to the deck. In this study, in order to consider the influence of only the bow flare angle on the green water phenomenon, the flare angle along the side of the deck is designed to be the same value as the conventional ship which has 90 degrees bow flare angle except for the bow flare angle. Fig 4 shows examples of the body plan according to the angle of the bow flare designed in this study. Also, the model of the FPSOs below free surface was kept equal and the bow flare angle was applied from above the free surface. In this study, the simulation was performed from 90 to 60 degrees while decreasing the bow flare angle by 15 degrees. The length of the deck was designed to be equal as the bow flare angle decreased to maintain the shape of the deck.

4.2 Wave conditions

The green water on the deck is mostly influenced by the relative motions of the ship and the wave of the incident waves. When there is an incident wave, the relative motion affected by the heave and pitch motions of the ship and the wave height of the incident wave around the bow is amplified when the wavelength of the incident wave is similar to the length of the hull and the wave steepness which is the ratio of wave height to wavelength is very large. A range of wave heights and wave periods/lengths was used to determine the sensitivity of the results for these parameters.

Wave steepness (H_W/λ)	Wave amplitude (A, cm)		
	λ = 225cm	λ = 300cm	λ = 375cm
0.04	4.500	6.000	7.500
0.05	5.625	7.500	9.375
0.06	6.750	9.000	11.25

Table 2 Wave conditions for the green water simulations.

According to reports of accidents caused by the green water to date, it was mentioned that the range of the wave steepness was 0.01 to 0.06, which caused many accidents due to the green water (Ersdal and Kvitrud, 2000; Leonhardsen et al., 2001). Therefore, considering these ranges, three wave steepness (0.04, 0.05 and 0.06) and three wavelengths (0.75, 1.0 and 1.25 times to the length of the ship) were used as wave conditions of this study. Because the main focus was on wave conditions where the wavelength (λ) is similar to the ship length (L) because in this range the most critical relative wave motions occur and it might result in larger green water phenomenon on the deck. ($0.75<\lambda/L<1.25$). The selected wave amplitudes (A_W) and wavelengths are listed above Table 2.

Also, the determined incoming wave is regular wave. And it can be used as a snapshot of a critical wave train in an irregular sea state. In this way the critical event is repeated and can be studied a number of times with controlled input waves.

5 Numerical modelling

This section will outline the numerical methods used in the CFD model and describe numerical approaches.

5.1 Governing equations

Apart from body forces, for incompressible flows, the momentum equations and averaged continuity are used in the form of tensor and the Cartesian coordinate system is as follows (Ferziger and Peric, 2002):

$$\frac{\partial(\rho\bar{u}_i)}{\partial x_i} = 0 \tag{1}$$

$$\frac{\partial(\rho\bar{u}_i)}{\partial t} + \frac{\partial}{\partial x_j}\left(\rho\bar{u}_i\bar{u}_j + \rho\bar{u}_i'\bar{u}_j'\right) = -\frac{\partial\bar{p}}{\partial x_i} + \frac{\partial\bar{\tau}_{ij}}{\partial\bar{\tau}_{ij}} \tag{2}$$

In which $\bar{\tau}_{ij}$ are the mean viscous stress tensor components, as shown in Eq. (3)

$$\bar{\tau}_{ij} = \mu(\frac{\partial\bar{u}_i}{\partial x_j} + \frac{\partial\bar{u}_j}{\partial x_i}) \tag{3}$$

And p is the mean pressure, $\bar{u}_i$ is the averaged Cartesian components of the velocity vector, $\rho\bar{u}_i'\bar{u}_j'$ is the Reynolds stresses, ρ is the fluid density and μ is the dynamic viscosity.

A finite volume method which discretises the integral formulation of the Navier-Stokes equations was used to model the fluid flow. The RANS solver uses the predictive and compensator approach to connect continuity and momentum equations.

5.2 Physics modelling

The turbulence model used in this study was a standard k-ε model, which has been currently the most widely used model (CD-Adapco, 2014). Also, as reported by Querard et al. (2008), it stated that the k-ε model is much more economical when

compared to other turbulence model in computation time. For example, in the case of the SST model, the calculation time was found to be approximately 25% longer.

In this study, the Volume of Fluid shorten to VOF method was used to express the free surface when there was either a flat wave or regular wave. CD-Adapco (2014) defines the VOF method as, "a simple multiphase model that is well suited to simulating flows of several immiscible fluids on numerical grids capable of resolving the interface between the mixture's phase". And this model is commonly used with the 6-DOF motion model for marine applications. The concept of a steadily-progressing periodic wave train is a convenient model that is used in coastal and ocean engineering applications to give flow velocities, pressures on deck and wave heights arise from waves. The main theories that have been used for the steady wave problem is Stokes theory, which is an explicit theory that is based on an assumption that the waves are not very steep. This theory is best suited to modelling waves in deeper water (CD-Adapco, 2014).

5.3 Computational domain and boundary condition

As computer computing facilities become more advanced and easier to use, CFD simulations can be quickly computed for more complex and non-linear problems.

When using CFD, initial conditions and boundary conditions should be defined according to the feature of the problem. Setting these boundary conditions plays a very importance role in obtaining accurate results. The number of cases that can be used as a boundary condition is a lot. However, setting appropriate boundary condition for each condition can reduce unnecessary computation time in calculation (Date and Turnock, 1999).

Fig. 5 shows the FPSO model in the computation domain and specifies the boundary conditions.

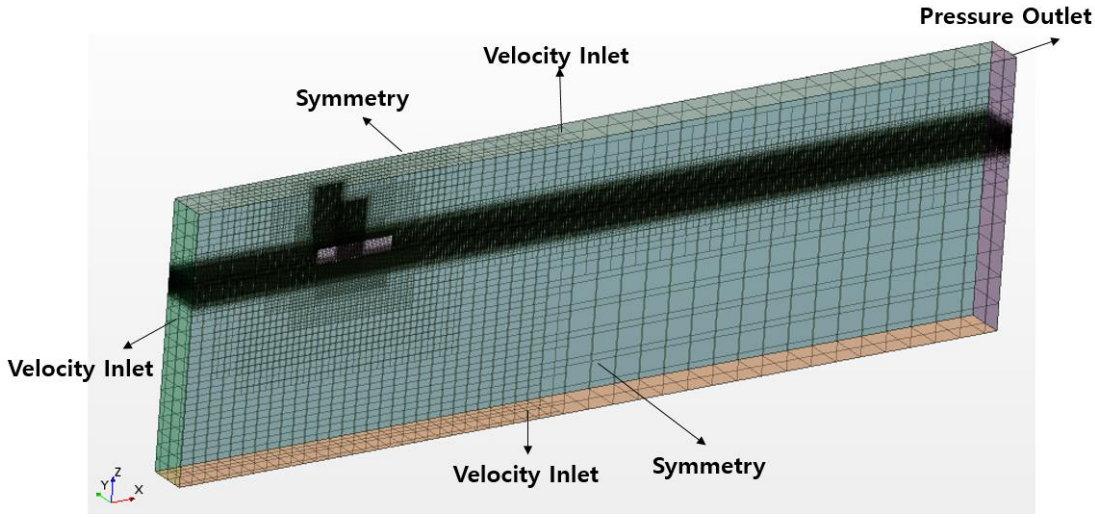

Figure 5 3D view of the background region and the applied boundary conditions.

In order to decrease the computation time, only half (the port side) of the FPSO model was calculated. In order to accurately simulate the starboard direction which is the other half of the model, a symmetry plane was formed based on the centre line of the ship.

In Fig. 5, the velocity inlet part forming the incident regular waves is formed in the negative x direction. The boundary condition of the outlet in positive x direction was set as a pressure outlet. Both top and bottom boundary conditions were set as velocity inlet and boundary conditions of symmetry plane and side were set as symmetry condition.

ITTC (2011b) recommends that when calculating simulations with incident regular waves, the inlet boundary should be located 1 to 2 times the ship length away from the vessel to obtain adequate results. It also states that the outlet boundary should be located 3 to 4 times the length of the ship so that it can be positioned farther away from the ship to prevent superposition due to the wave reflected from the outlet boundary.

Fig 6 shows the location of each boundary away from the ship and is represented by the front and side views of the domain. As I mentioned in Section 3.1, the use of the fixed model does not affect the results even with the truncated model, so the model is used at 1.5m length, which is half of the total length of the ship. In STAR-CCM+, when the VOF model uses, there are VOF wave damping function and VOF wave

forcing function to prevent reflection wave from outlet boundary. In this study, VOF wave damping function was used in all cases and damping length is twice the wavelength. The distance from the VOF wave damping-enabled boundary at which the damping starts. The specified value must be at least one wavelength (CD-Adapco, 2014).

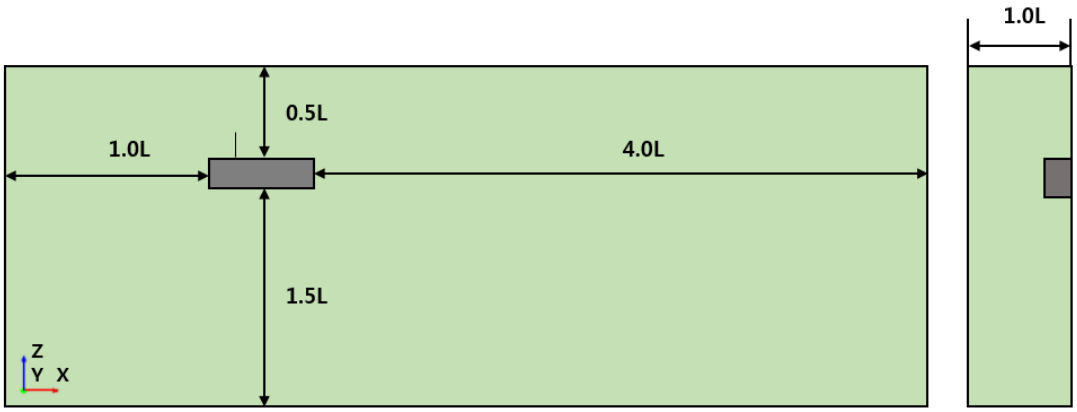

Figure 6 The dimensions of the computational domain for the green water simulations: (left) Side view, (right) front view.

5.4 Coordinate system

The flow field was solved, and the green water loads and wave height on the deck were calculated in the earth-fixed coordinate system.

5.5 Mesh generation

Mesh generation was formed using the automatic meshing function in STAR-CCM+, which uses the Cartesian cut-cell method. For complex mesh generation problems, a trimmed cell mesher was used to create a high quality grid. Since the number of cells varies with wavelength and wave height, the total number of girds is different for each case.

In order to simulate FPSO in waves, the mesh was generated along the guidelines provided by the ITTC (2011b) for the CFD application. According to these guidelines,

a minimum of 80 cells per wavelength should be used and a minimum of 20 cells per wavelength should be used in the area where free surface is expected to from. So in this study, 100 cell per wavelength were used and 30 cell per wave height were used to capture the green water on the deck. And in order to capture the severe green water phenomenon around the deck, it was generated using the same size as the grid around the free surface in the both x direction and z direction where the green water phenomenon was expected. Fig. 7 represents the volumetric mesh around green water zone and free surface. Additionally, Fig. 8 represents the surface mesh on the deck. In this study, the deck which is located in front of the superstructure is called front deck and the deck which is located behind the superstructure is called rear deck when the surface mesh is generated to measure the pressure of green water on the deck. Because the pressure and water height are measured on the front deck, the surface mesh of the front deck is densely generated and the surface mesh of the rear deck is not densely generated to reduce the computation time. Also, when generating surface mesh of the superstructure, it was densely generated in the same size as the front deck to measure the pressure of green water on the superstructure.

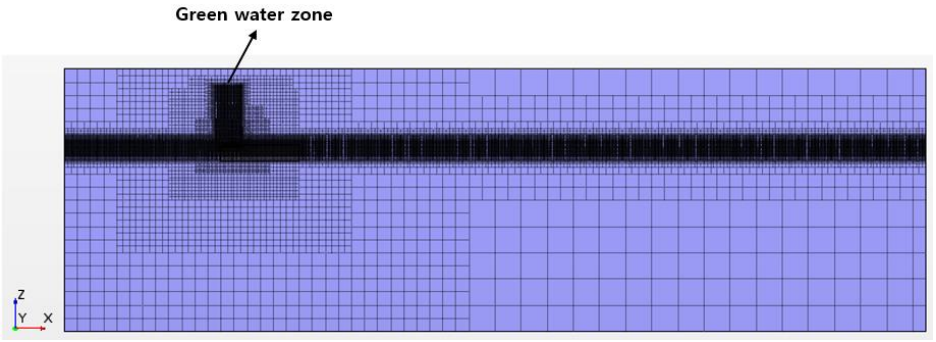

Figure 7 Volumetric mesh around green water zone and free surface.

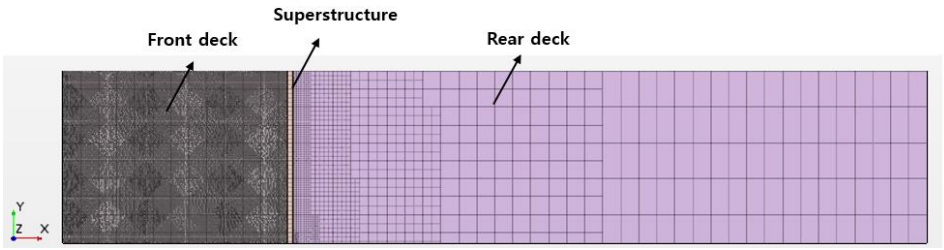

Figure 8 Surface mesh on the deck.

5.6 Post-processing formulations

This section will describe the expression used during processing of the results before moving to the results and discussion sections.

To begin with, weighted arithmetic mean was used to analyse the pressure and water level on the deck when the green water occurred. The pressure applied at each position was calculated as a ratio to the overall pressure of the deck, and the ratio was set as a weighted coefficient at each position, so that the overall pressure applied to the deck was compared with other design hulls. The weighted arithmetic mean is similar to the most common arithmetic mean used, however, instead of each data point contributing equally to the final average, some data points contribute more than other data points.

Formally, the weighted mean of a non-empty set of data {P11, P12, ⋯, P44}, where P represents a set of mean value with non-negative weights.

$$\overline{\mathrm{P}} = \frac{\sum_{i=1,j=1}^{i=4,j=4} w_{ij} P_{ij}}{\sum_{i=1,j=1}^{i=4,j=4} w_{ij}} \tag{4}$$

Which means:

$$\overline{\mathrm{P}} = \frac{w_{11}P_{11}+w_{22}P_{12}+\cdots+w_{44}P_{44}}{w_{11}+w_{22}+\cdots+w_{44}} \tag{5}$$

Therefore, elements with larger weights have a greater impact on the weighted mean than elements with smaller weights. The weight cannot have a negative value. Some can be zero, but it is impossible for all values to have zero. The water level on the deck is also measured by weighted arithmetic mean method.

6 Results

This section will describe the simulation results obtained from this study, and will also show the results the compared with the experimental results (Hyun-ho et al., 2012). It will then compare the conventional ship which has 90 degrees bow flare angle with the design ships which have 75 and 60 degrees bow flare angle and discuss the results. Validating CFD results against EFD results is a necessary process before comparing these results.

6.1 Validation

Due to the highly non-linear and complexity for the green water phenomenon, it is important to compare the experimental results with the simulation results. This can be used to verify the simulation results and approach.

6.1.1 Wave generation

In this study, 5^{th}-order stokes waves were used to create a regular wave in all simulations. This wave was used according to what CD-Adapco (2014) mentioned, "this wave more closely resembles a real wave than one generated by the first order method". The first order wave mentioned here is the wave that generates a regular periodic sinusoidal profile. In order to identify the wave generated from the inlet boundary, the wave elevation was recorded by installing a wave probe at 0.5 times the wavelength from the inlet boundary in all cases and Fig. 9 show the location of numerical wave probe to record the incident wave elevation. Fig. 10, as an example, displays the recorded time history of the wave elevation at the probe, which has the shortest wavelength among all cases and the wave height when the wave steepness is 0.05.

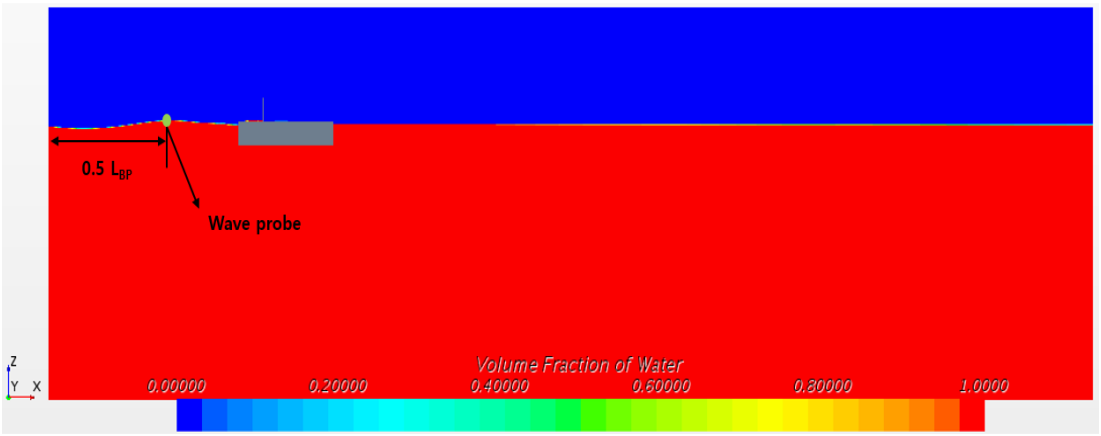

Figure 9 Numerical wave probe to record the wave elevation.

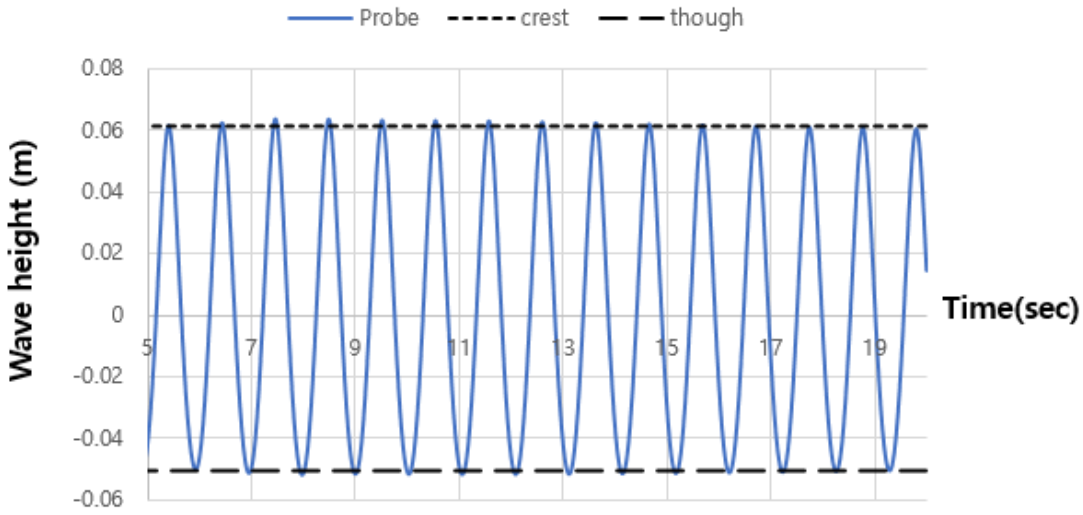

Figure 10 Time series graph of wave elevation at the numerical wave probe.

In Fig. 10 a blue solid line represents wave elevation at the probe and two dotted lines represent a crest and though in the stokes 5th waves, respectively. And the mean of the 1st harmonic wave amplitudes covering from 5 seconds to the end was calculated to be 0.0637m, which under-predicts the actual stokes 5th waves amplitude which is 0.0614m by 3.72%. This slight difference in wave amplitude can be judged to be appropriate for the cell size and time step of the current using and it can be said that it has been sufficiently verified for wave generation in the CFD model.

6.1.2 Validation of pressure values on deck

In the case of FPSO models which have different bow flare angle, there were ten points on the front deck for pressure measurement shown in Fig. 11 below.

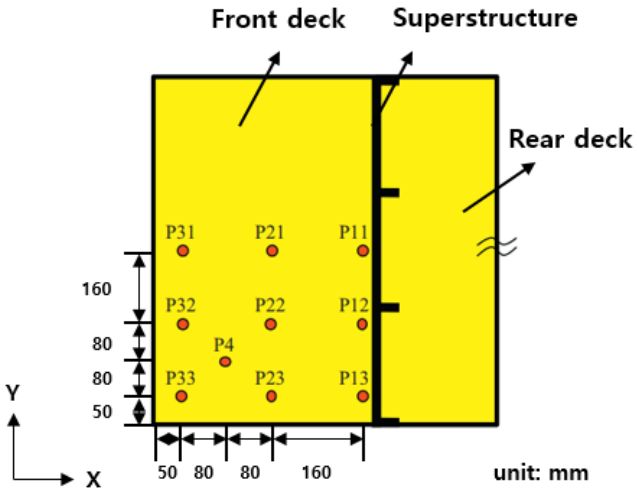

Figure 11 Location of pressure measurement on the deck.

Fig. 12 below graphically shows the maximum pressure of the model test and numerical calculation in 3 different wave steepness. Firstly, when the wave steepness is 0.06 (a), it can be seen that there are less errors in the positions of P31, P32, P33 and P4 at the end of the deck. However, it can be seen that there are more errors at the locations near the superstructure because once the wave hits the superstructure and then wave breaks, which is considered to be due to its nonlinearity and complexity. It is considered that a finer grid on the deck should be formed in order to reduce errors caused by nonlinear causes. Secondly, when the wave steepness is 0.05 (b), As a whole, it can be confirmed that the CFD value is measured to be smaller than the EFD value. Numerically, as in other cases, there is a bit large difference at the point near the superstructure, and a little difference at the point at the end of the deck. Lastly, when the wave steepness is 0.04 (c) which is the smallest wave steepness in wave conditions, it can be seen that the difference between EFD and CFD is larger than the other cases numerically. And (b) and (c), the wave steepness is calculated for the case where the

wavelength of (c) is longer than the wavelength of (b) when the wave heights are the same. Therefore, in case of (c), the pressure values for all locations are smaller than (b) although wave steepness is low.

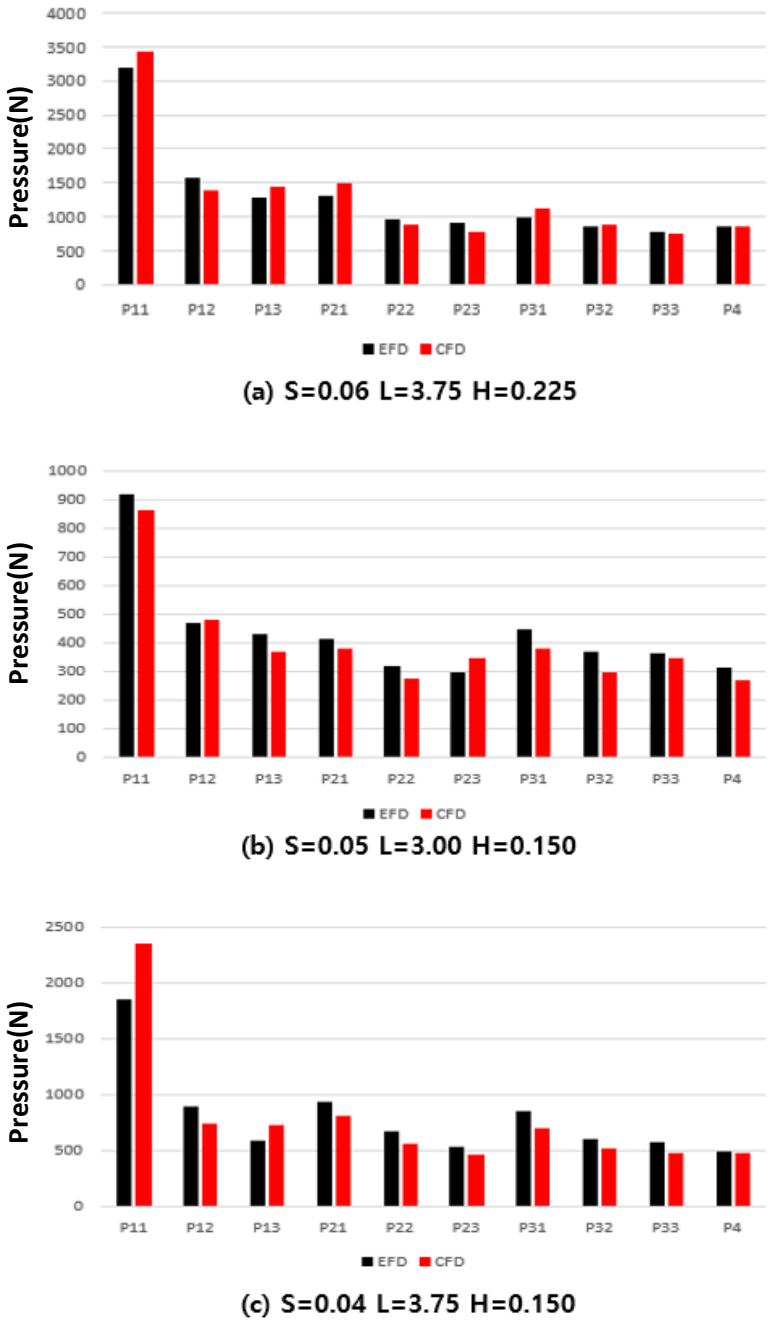

Figure 12 3 cases of maximum pressure comparison between EFD and CFD results each wave steepness (S: wave steepness, L: wavelength, H: wave height).

Table 3 shows the maximum pressure values of EFD and CFD and the error rates of EFD and CFD at each measurement point in order to quantitatively compare the EFD and CFD results. When the wave steepness is 006, It can be confirmed that the error rate is within 15% in entire section. As mentioned earlier, the error rate is within 3% at the measurement points located at the end of the deck, but the error rate increases gradually toward the superstructure. However, when the wave steepness is 0.05, the P32 which is located at the end of the deck shows the largest error rate because the absolute numerical value of the pressure has a relatively smaller value than the measurement positions near the superstructure. Lastly, when the wave steepness is 0.04, it is shown that the error rate is within about 25% in whole section. As mentioned before, it can be seen that the error rate increases as the wave steepness becomes smaller. This tendency is also shown because the absolute value of the pressure measured on the deck is significantly smaller than when the wave steepness is smaller. In order to reduce this error, it can be assumed that the gird on the deck can be formed more densely to obtain better results.

Location	Wave steepness=0.06			Wave steepness=0.05			Wave steepness=0.04		
	EFD (Pa)	CFD (Pa)	Error (%)	EFD (Pa)	CFD (Pa)	Error (%)	EFD (Pa)	CFD (Pa)	Error (%)
P11	3182	3421	7.51	917	862	5.91	1842	2348	27.48
P12	1560	1393	10.71	469	478	2.05	888	735	17.12
P13	1271	1431	12.58	431	365	15.16	586	730	24.63
P21	1308	1490	13.91	412	377	8.33	937	808	13.67
P22	953	875	8.12	318	274	13.63	672	562	16.31
P23	899	768	14.54	295	347	17.93	528	460	12.88
P31	994	1110	11.67	446	377	15.45	844	698	17.20
P32	863	880	2.03	369	293	20.49	601	510	15.08
P33	770	750	2.47	364	344	5.39	575	472	17.84
P4	866	867	0.14	310	267	13.71	482	478	0.70

Table 3 Comparison of the percent relative error about maximum pressure between EFD and CFD results in 3 cases.

6.2 Simulation results

This section will describe the simulation results accomplished in this study and it is divided into five sub-section, each of which presents different aspects of findings.

6.2.1 Green water behavior

In this study, the green water phenomenon on the deck of the FPSO model caused by the incident waves is analyzed with using CFD simulations. Fig 13 shows the process of the green water phenomenon in one period divided into 8 phases. First of all, when the wave reaches the bow of the ship, the direction of wave movement is deformed vertically. And then air between the wave front and the bow of the ship is entrapped. The third step shows that the water level in front of the bow of the ship increases rapidly and waves fall on the deck which causes the maximum pressure in a period. After that, it moves along the deck until it reaches the superstructure. When the wave reaches the superstructure, the direction of the wave changes vertically again to form a high water column. At this time, the biggest force is applied to the superstructure. After that, the formed water column collapses and falls back on the deck again, causing the secondary maximum pressure. Thereafter, there is no further ingress of water, so it is the phase that the water on top of the deck exits. Lastly, as the water remaining on the deck exits and affects the wave of the next incident wave. It can be confirmed that the wave elevation is continuously changed every period in front of the bow due to the superposition of the incident wave and the water drainage from the deck. Fig 14 is a time series graph showing the wave height measured by installing a wave probe right in front of the bow of the ship. As shown in the graph, the wave elevation continues to change. Due to this phenomenon, the maximum value of the pressure on the deck is measured differently for each period.

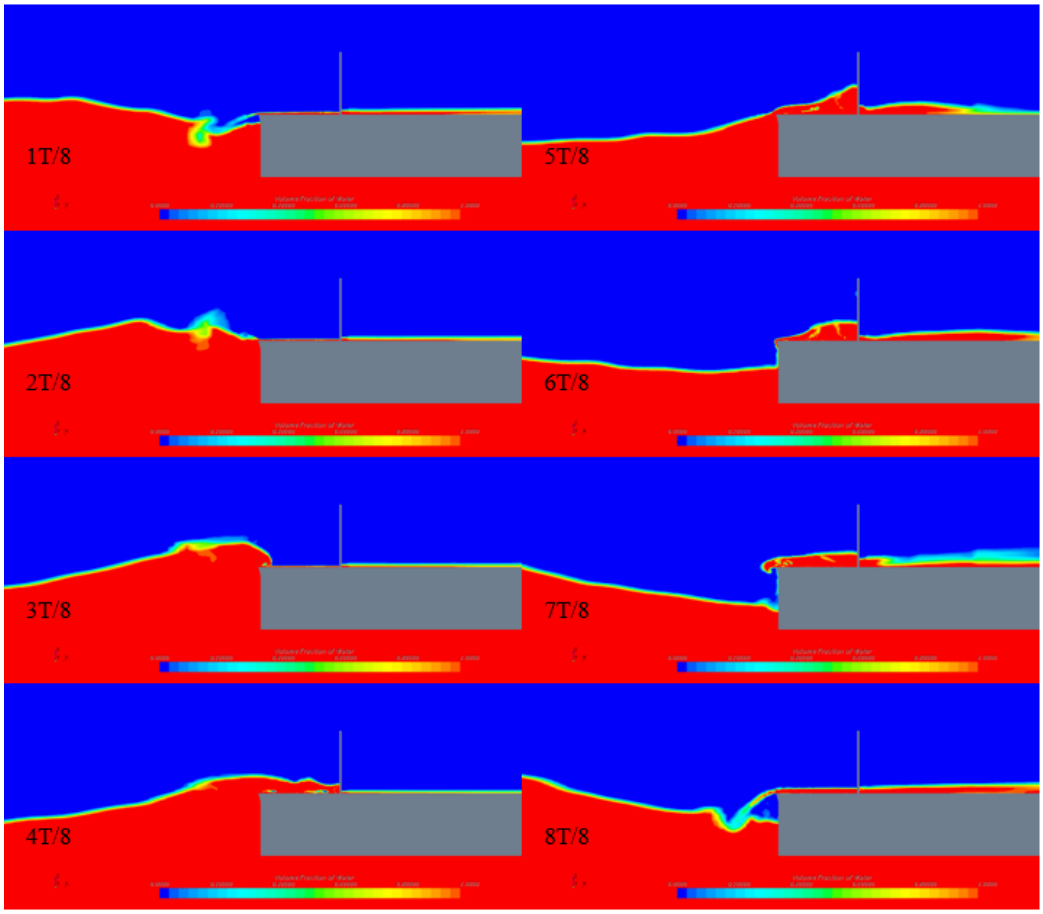

Figure 13 Volume of fluid (VOF) scene of CFD simulation on green water phenomenon.

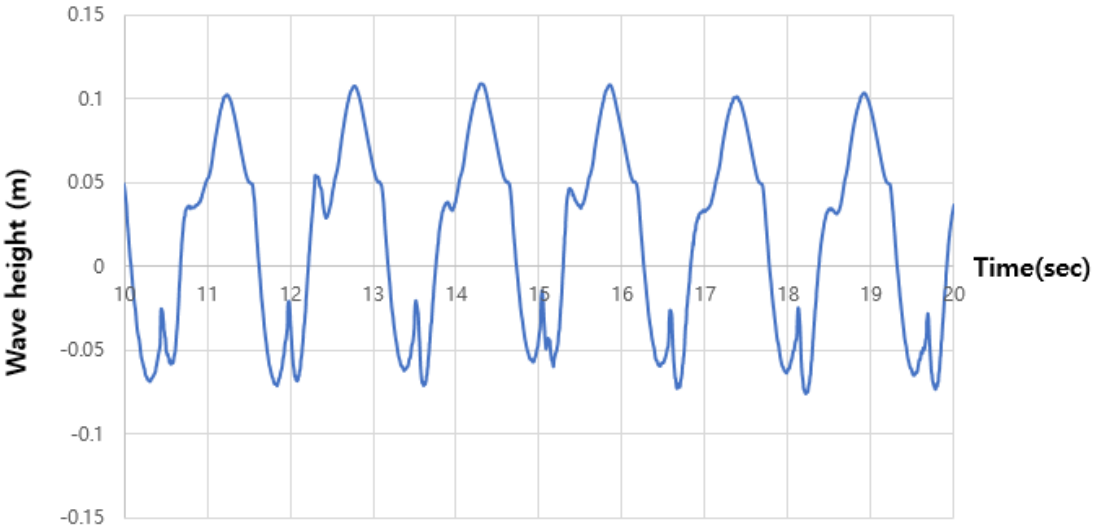

Figure 14 Time series graph of wave height at the numerical wave probe which is located right in front of the bow.

Figures 15 through 17 show the process of the green water phenomenon in a period according to the bow flare angle when the wave steepness is the largest case which is 0.06 and the wavelength and the wave height are 3.75m, 0.225m, respectively. First of all, it can be seen that the water column is formed higher than the superstructure height after the waves hit the superstructure at all bow flare angles. However, it can be seen that the wave height beside the deck at the third moment of the 8th divided cycle when the bow flare angles are 75 and 60 degrees is lower than that of the 90 degrees. This is expected to reduce the amount of water ingress the deck side and also decrease the water level on the side of the deck. Also, in the case of water drainage at the last moment, it can be seen that the ship which has 90 bow flare angles is slower than other design ships which have 75 and 60 bow flare angles.

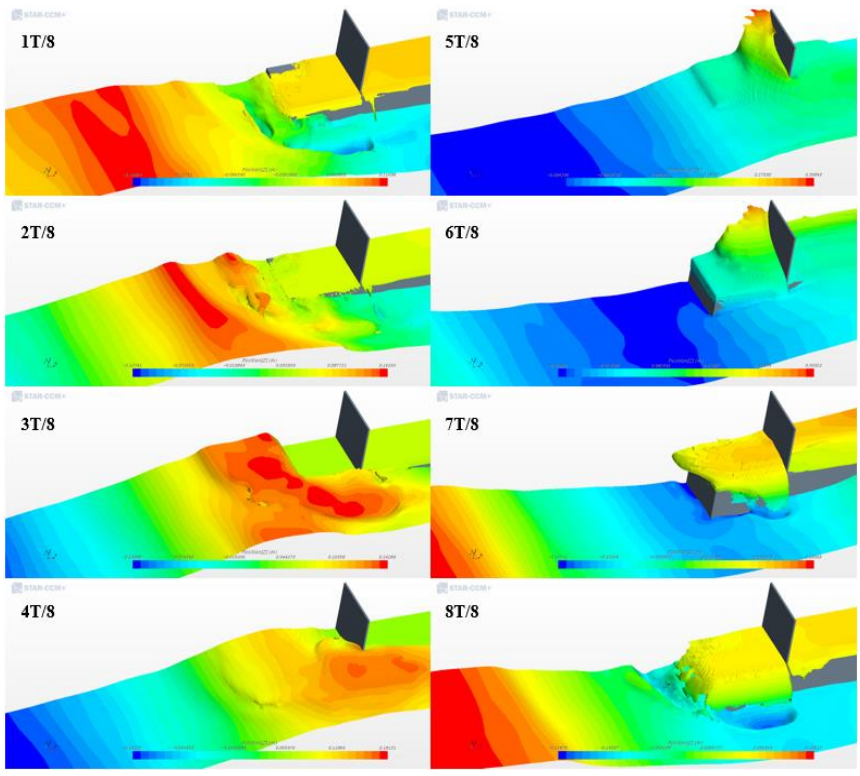

Figure 15 3D Scenes of the generation of green water when the bow flare angle is 90 degrees in wave condition (S=0.06, λ =3.75, H=0.2250).

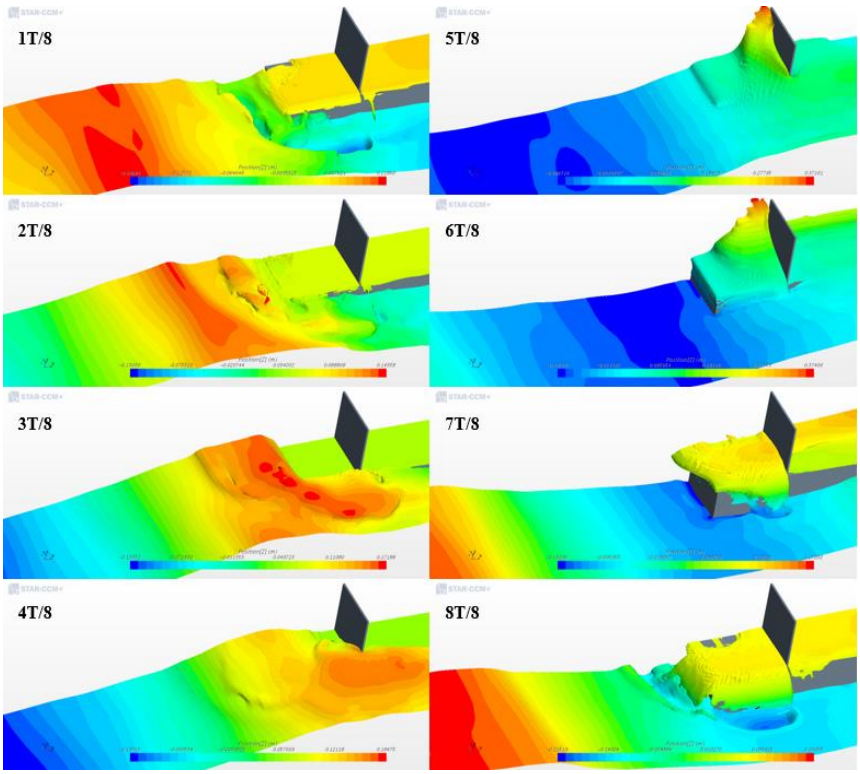

Figure 16 3D Scenes of the generation of green water when the bow flare angle is 75 degrees in wave condition (S=0.06, λ =3.75, H=0.2250).

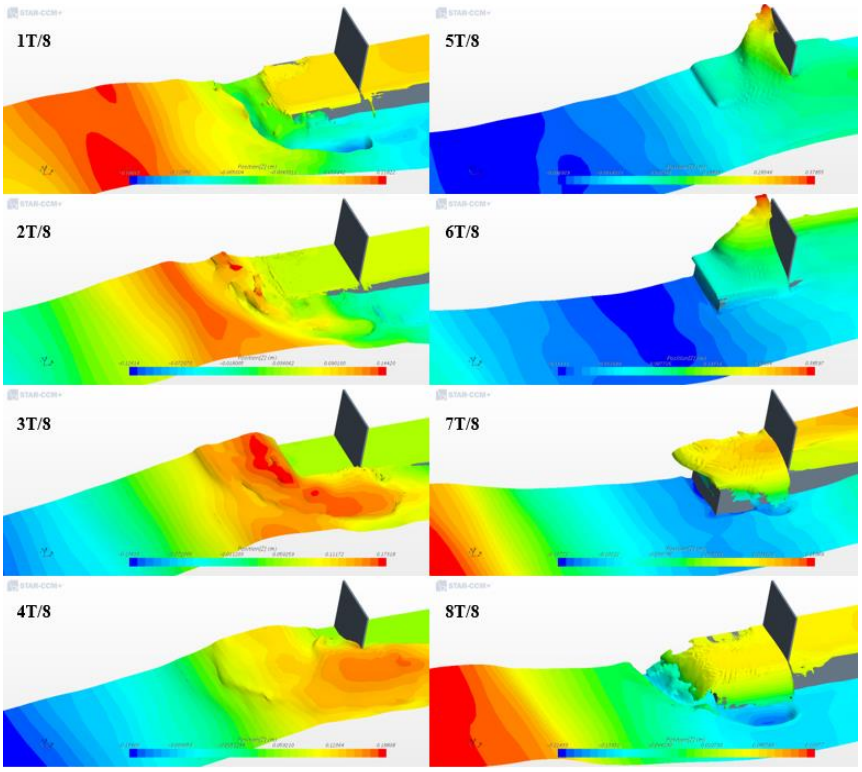

Figure 17 3D Scenes of the generation of green water when the bow flare angle is 60 degrees in wave condition (S=0.06, λ =3.75, H=0.2250).

Figures 18 through 20 show the process of the green water phenomenon in a period according to the bow flare angle when the wave steepness is 0.05 and the wavelength and wave height are 3.75m, 0.1875m, respectively. As before, it can be seen that the wave height beside the deck at the third moment of the 8th divided cycle when the bow flare angles are 75 and 60 degrees is lower than that of the 90 degrees. This is expected to reduce the amount of water ingress the deck side and also decrease the water level on the side of the deck. This is also expected to reduce the amount of water ingress the deck side and also decrease the water level on the side of the deck. However, when the water is drained at the last moment, there is no big difference. And when a wave is moved along the deck, it collides with the superstructure, and it is confirmed that the water column is formed by about half of the height of the superstructure.

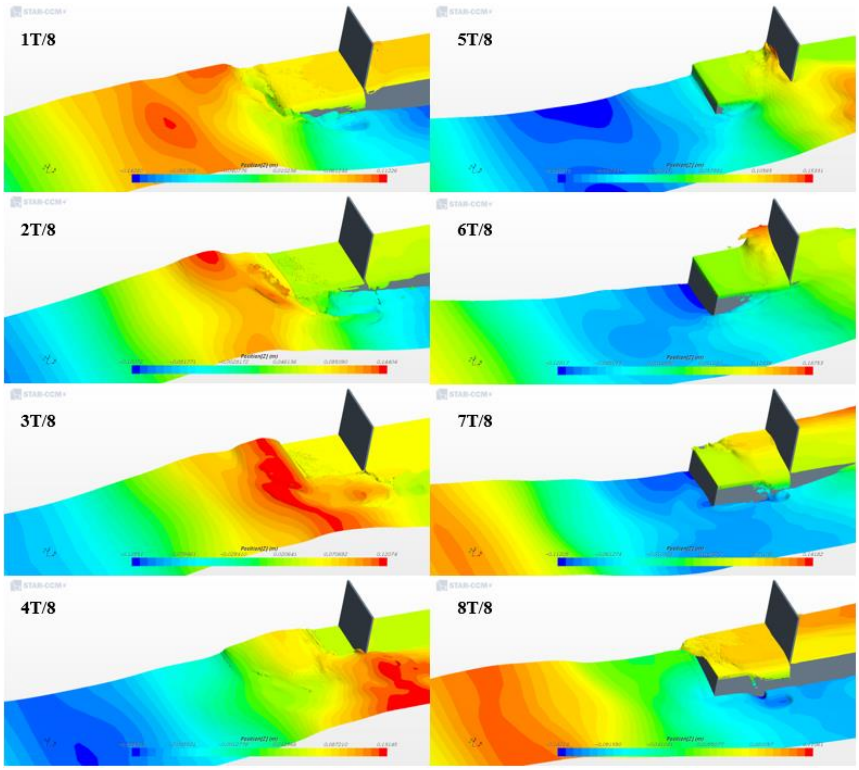

Figure 18 3D Scenes of the generation of green water when the bow flare angle is 90 degrees in wave condition (S=0.05, λ =3.75, H=0.1875).

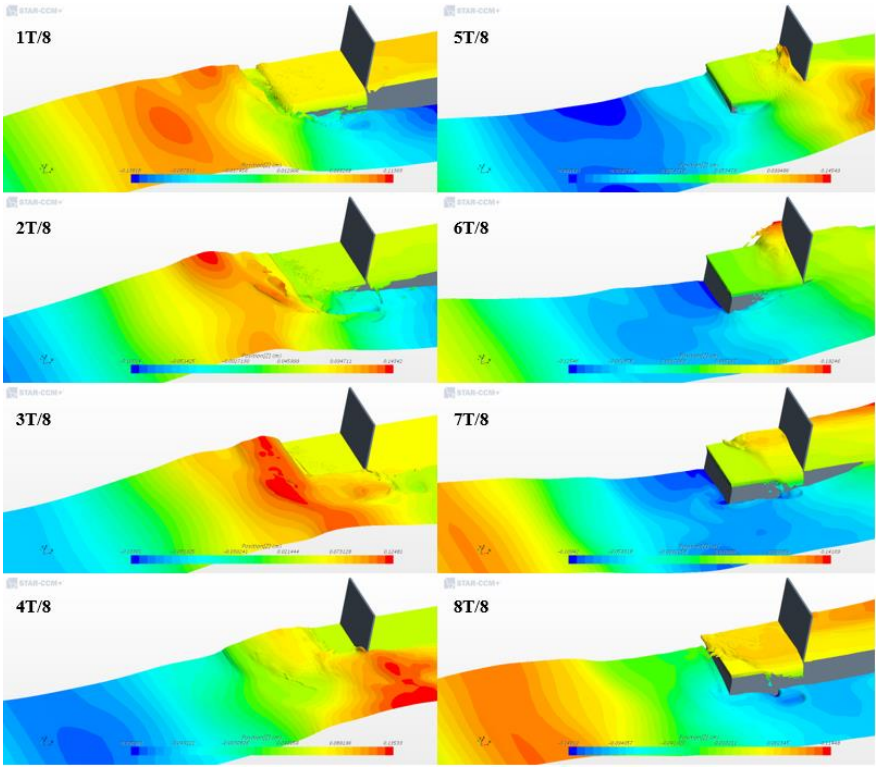

Figure 19 3D Scenes of the generation of green water when the bow flare angle is 75 degrees in wave condition (S=0.05, λ =3.75, H=0.1875).

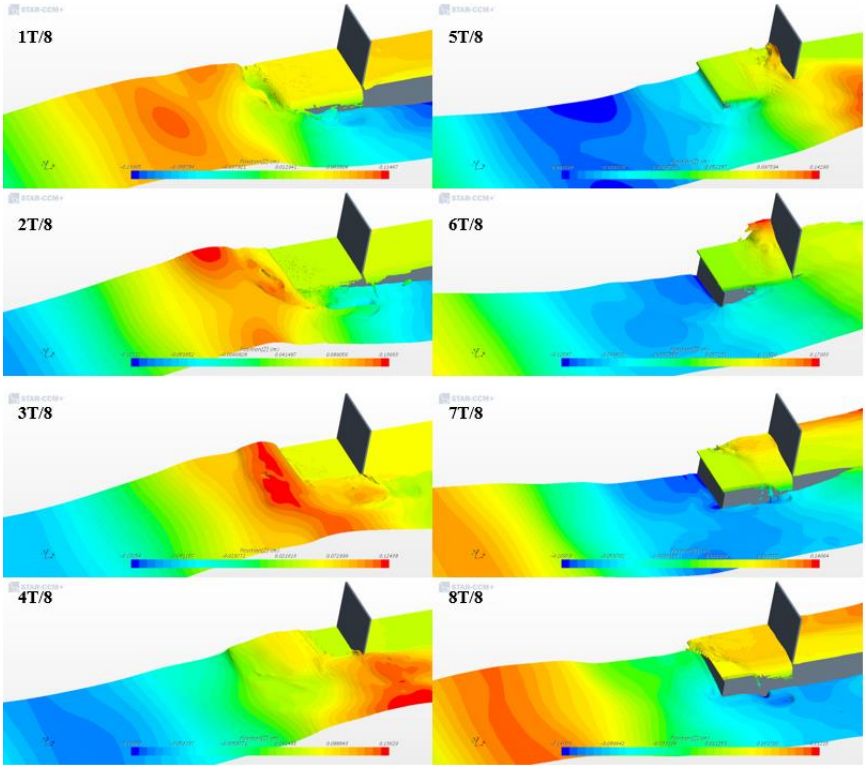

Figure 20 3D Scenes of the generation of green water when the bow flare angle is 60 degrees in wave condition (S=0.05, λ =3.75, H=0.1875).

Figures 21 through 23 show the process of the green water phenomenon in a period according to the bow flare angle when the wave steepness is the smallest case which is 0.04 and the wavelength and wave height are 3.75m, 0.15m, respectively. In this case of the wave steepness, it can be seen that the water column formed in front of the superstructure is small compared to the case where the wave height is larger than that before. However, when the waves approach the bow of the ship, due to the influence of the bow flare angle, the smaller the bow flare angle, the lower the water level right next to the deck is.

In summary, the wave height next to the deck when the bow flare angles are 75 and 60 degrees, regardless of the wave steepness, is lower than that when the bow flare angle is 90 degrees and the amount of water ingress the deck decreases. This effect can be expected to reduce the pressure on the deck and also decrease the force on the superstructure.

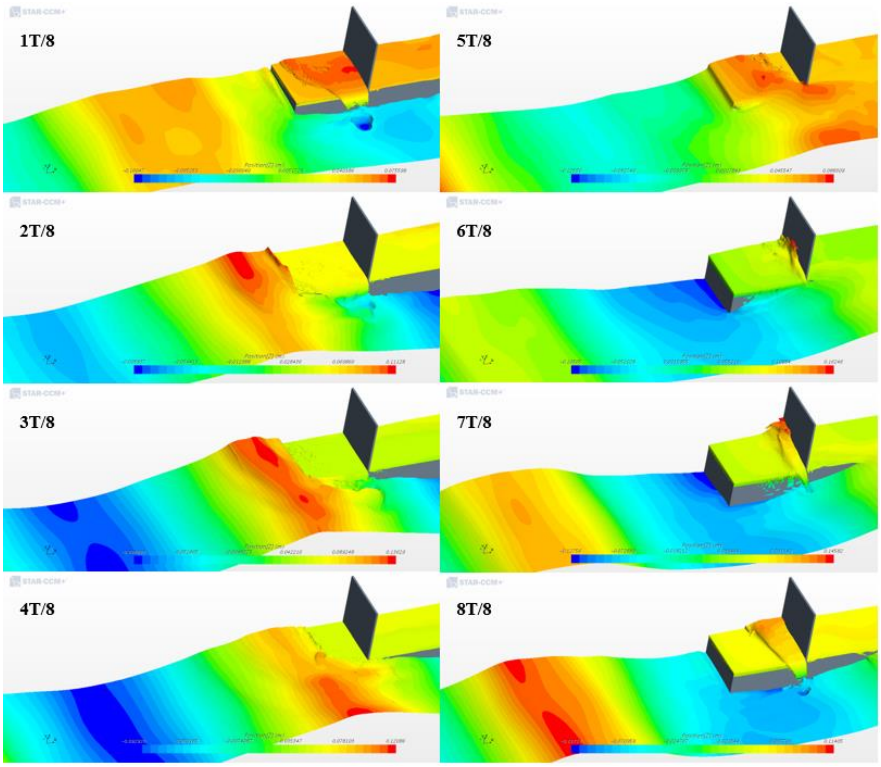

Figure 21 3D Scenes of the generation of green water when the bow flare angle is 90 degrees in wave condition (S=0.04, λ =3.75, H=0.1500).

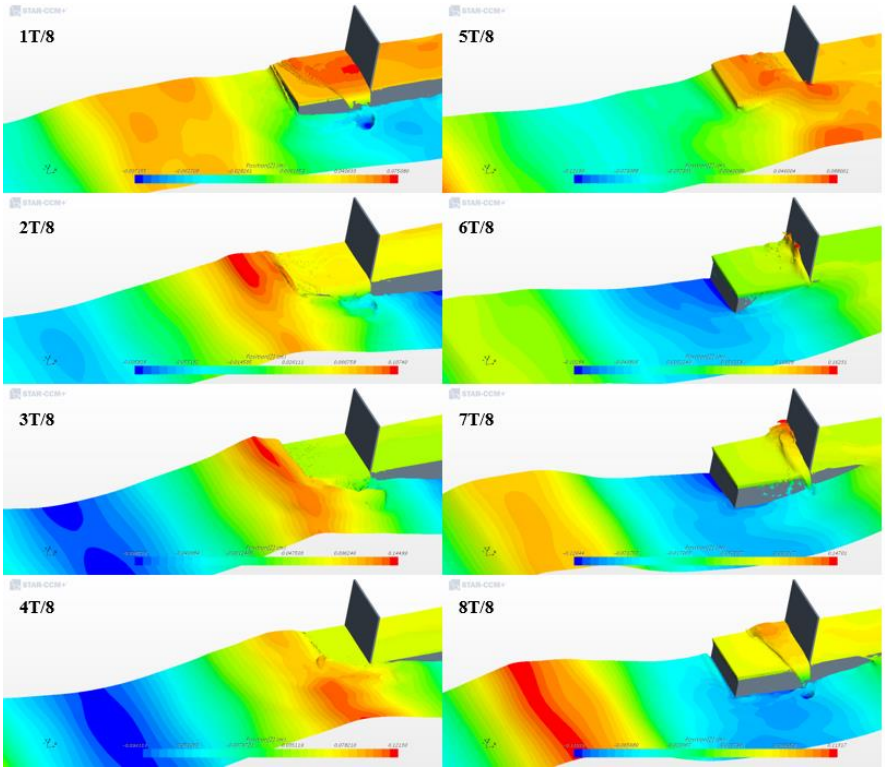

Figure 22 3D Scenes of the generation of green water when the bow flare angle is 75 degrees in wave condition (S=0.04, λ =3.75, H=0.1500).

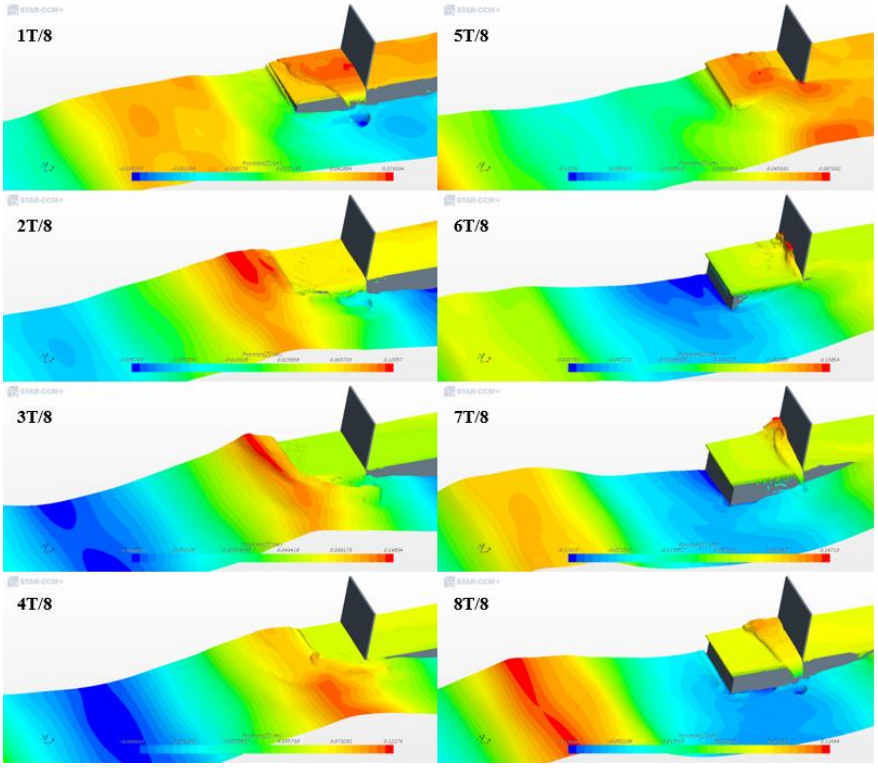

Figure 23 3D Scenes of the generation of green water when the bow flare angle is 60 degrees in wave condition (S=0.04, λ =3.75, H=0.1500)

6.2.2 Water level on deck

As mentioned before section, the effect of the bow flare angle showed a tendency that the wave height at the side of the deck was lowered after the wave hit the bow of the ship. Figures 24 and 25 show the comparison from the moment the waves reached the edge of the bow to the moment the water entered the deck. One period when the green water occurs is divided into 16 equal parts, and only 5 of them each bow flare angle are shown below.

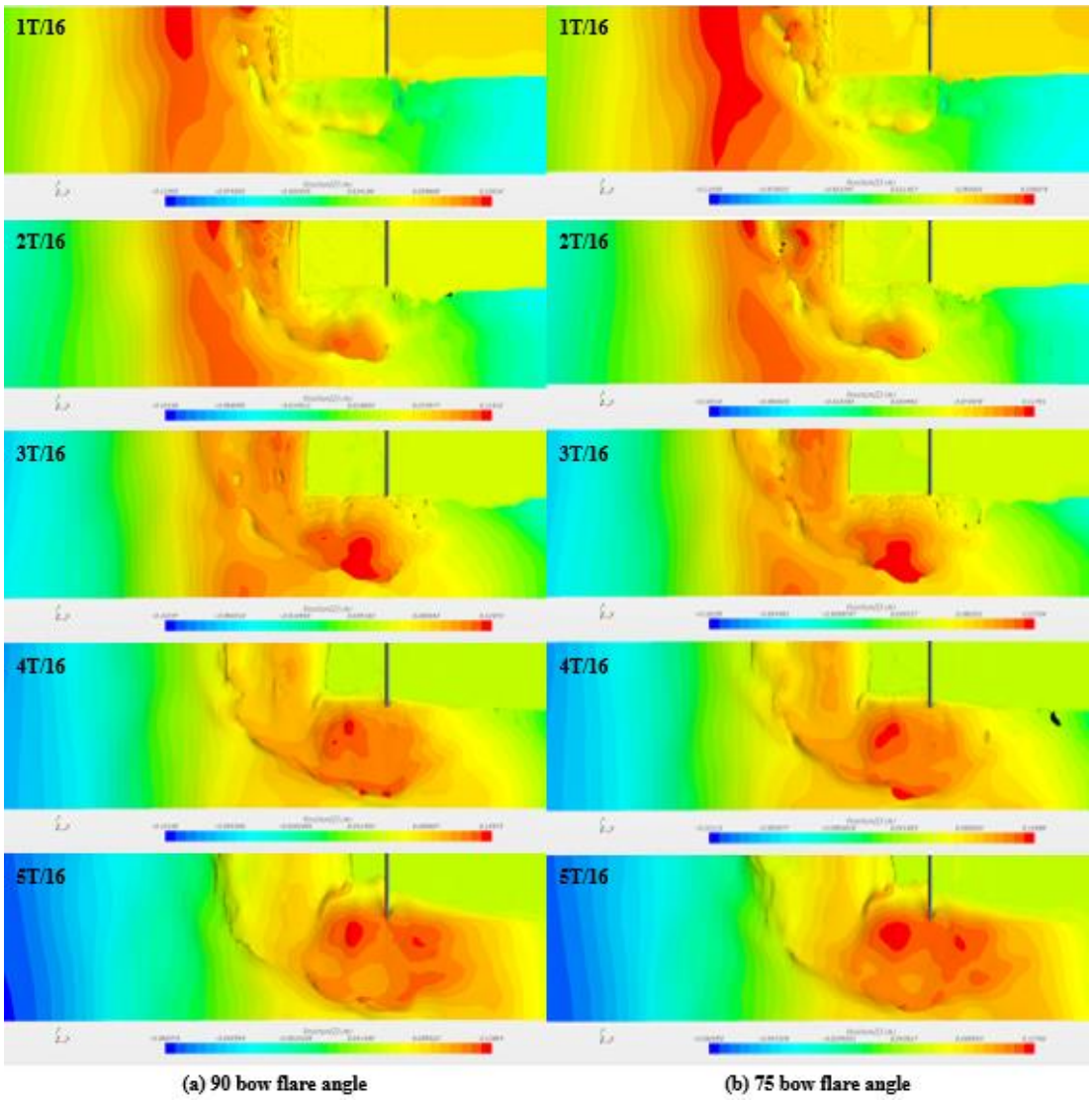

Figure 24 Top views around the FPSO which has 90 and 75 bow flare angles when the green water occurs (S=0.04, λ =3.75, H=0.1500).

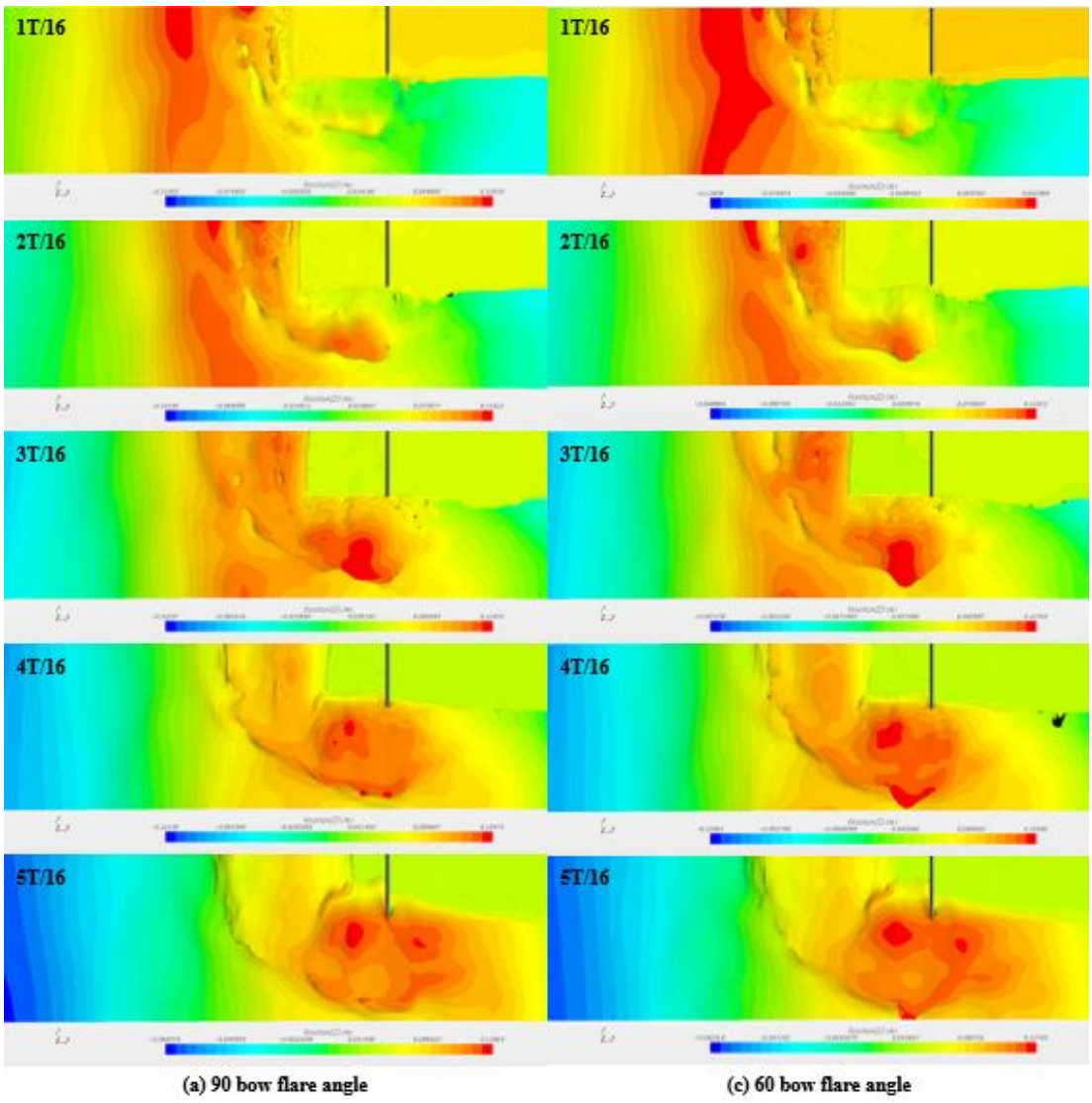

Figure 25 Top view around the FPSO which has 90 and 60 bow flare angles when the green water occurs (S=0.04, λ =3.75, H=0.1500).

In figure 24, (a) the left five pictures shows the top views of the wave height around the bow of the ship when the bow flare angle is 90 degrees and (b) the right pictures are when the bow flare angle is 75 degrees. When the bow flare angle is 90 degrees, it has a maximum wave height next to the deck which is 0.129m, but when the bow flare angle is 75 degrees, it has a maximum wave height next to the deck which is 0.127m. It is decreased by 1.5%. Also, as shown in figure 25, when the bow flare angle is 60 degrees, it is shown to be reduced by 2.2% from the bow flare angle of 90 degrees.

Figures 26 through 35 show the time series graphs of the water level on the deck each position for one period when the wave steepness is 0.04, the wavelength is 3.75m and the wave height is 0.15m. The x axis represents physical time and the y axis represents water level on the deck. The black solid line represents the hull which has bow flare angle of 90 degrees, the blue dash line represents 75 degrees and the red dash line represents 60 degrees. Each location for measuring pressure is mentioned in section 5.1.2.

When the bow flare angle is applied at P13 and P23 which are located side of the deck, it can be confirmed that the water level is decreased compared to the hull which has the bow flare angle of 90 degrees. However, at P31 and P32 which are located at the front of the deck, it can be seen that water levels are almost similar. It can be concluded that the bow flare angle does not reduce the amount of water entering the front of the deck but can decrease the amount of water that sideways penetrates. As the amount of water coming from the side of the deck decreases, the amount of water collected at the center of the deck decreases, so that the water level at P11 and P12 which are located right in front of the superstructure decreases when the bow flare angle is applied.

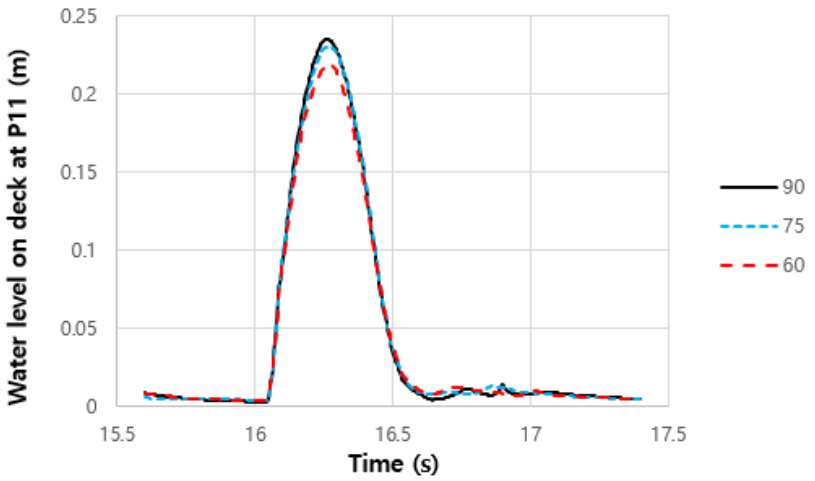

Figure 26 Comparison of the water level time histories at P11 (S=0.04, λ =3.75, H=0.1500)

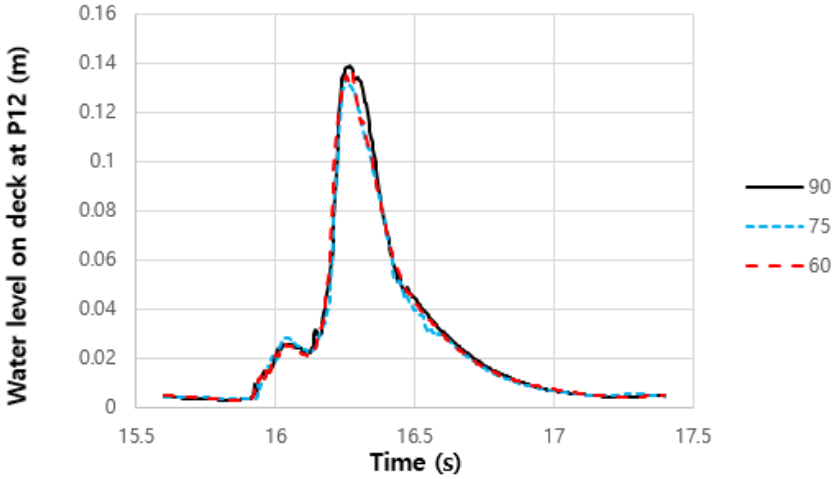

Figure 27 Comparison of the water level time histories at P12 (S=0.04, λ =3.75, H=0.1500)

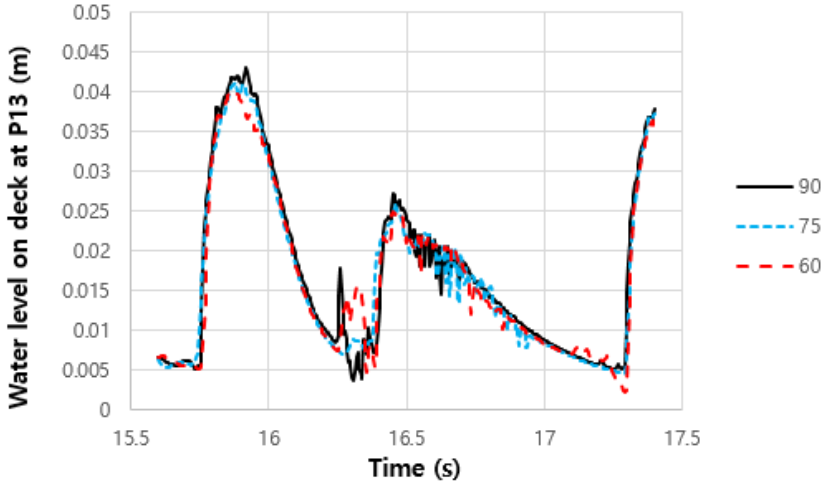

Figure 28 Comparison of the water level time histories at P13 (S=0.04, λ =3.75, H=0.1500)

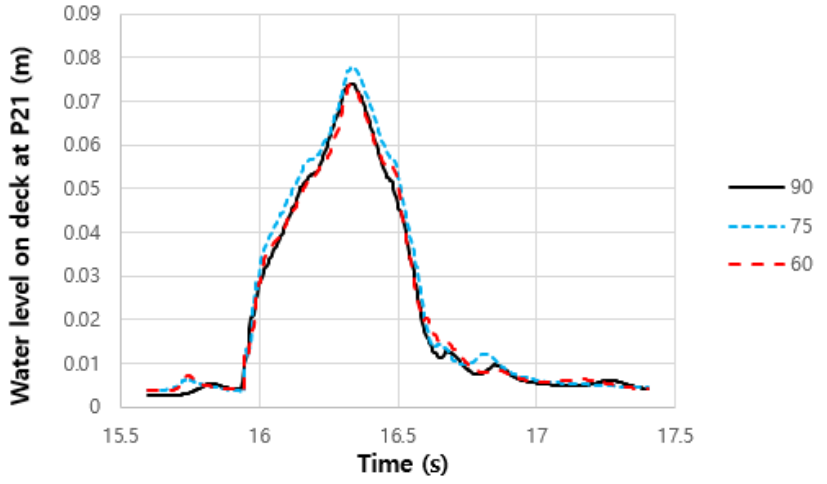

Figure 29 Comparison of the water level time histories at P21 (S=0.04, λ =3.75, H=0.1500)

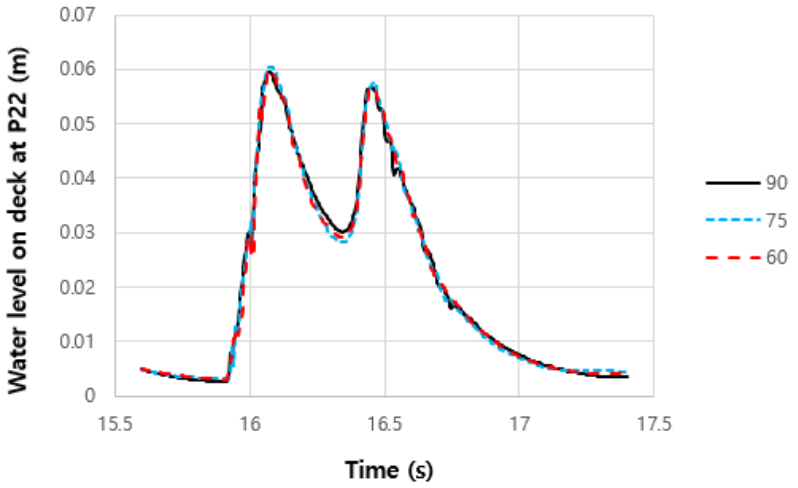

Figure 30 Comparison of the water level time histories at P22 (S=0.04, λ =3.75, H=0.1500)

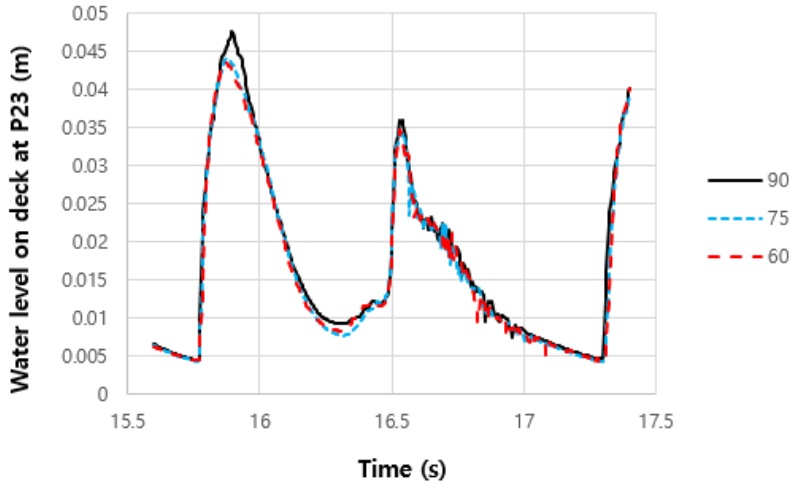

Figure 31 Comparison of the water level time histories at P23 (S=0.04, λ =3.75, H=0.1500)

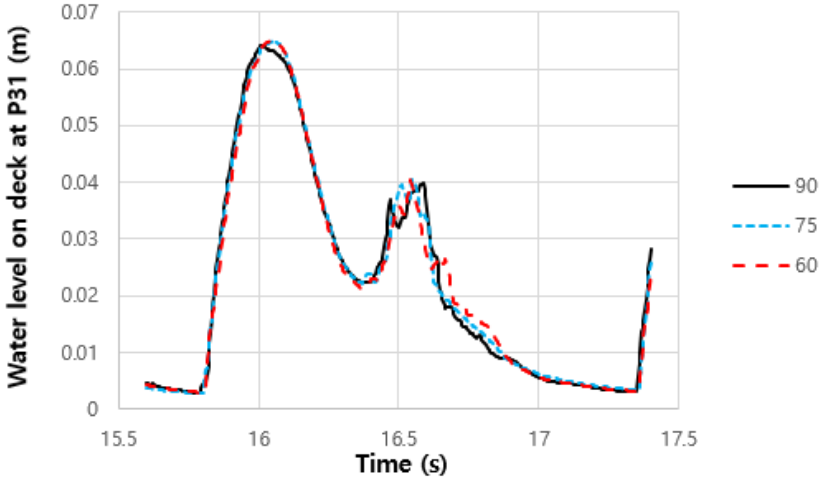

Figure 32 Comparison of the water level time histories at P31 (S=0.04, λ =3.75, H=0.1500)

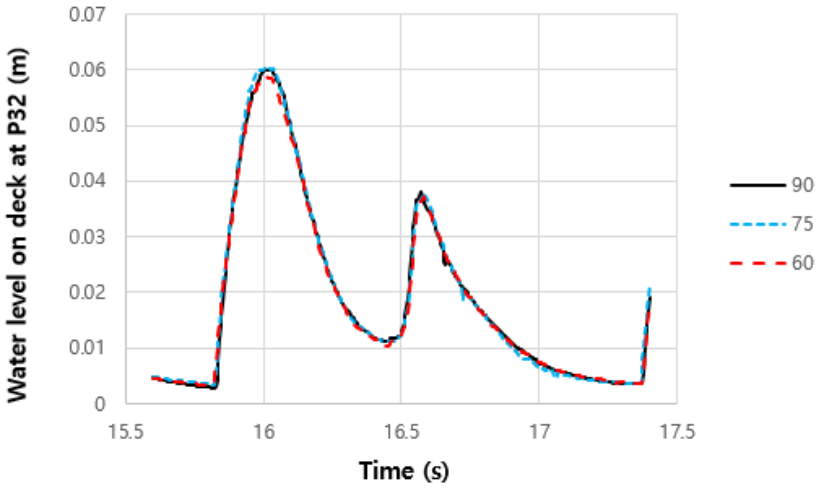

Figure 33 Comparison of the water level time histories at P32 (S=0.04, λ =3.75, H=0.1500)

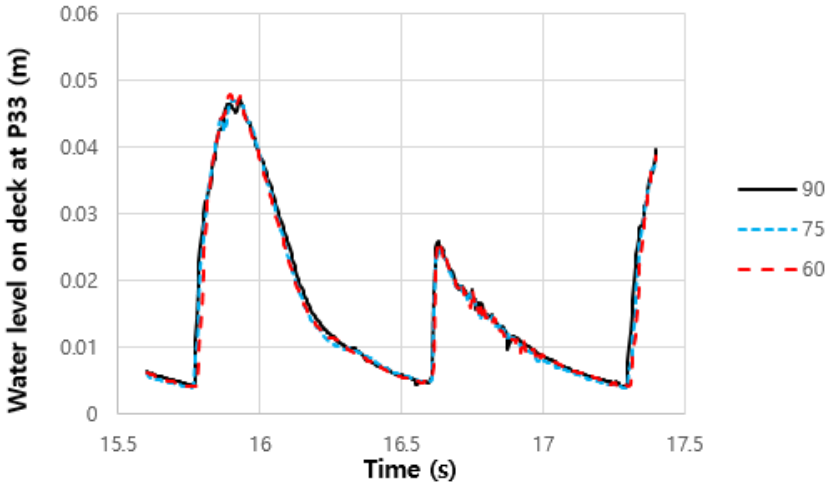

Figure 34 Comparison of the water level time histories at P33 (S=0.04, λ =3.75, H=0.1500)

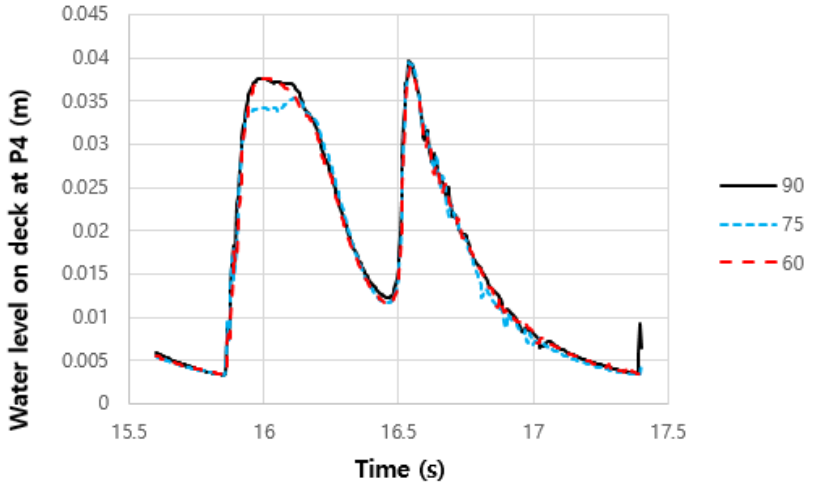

Figure 35 Comparison of the water level time histories at P4 (S=0.04, λ =3.75, H=0.1500)

Figures 36 through 38 below show the water level on the deck according to the wave steepness obtained using weighted mean. The x axis represents the wavelength and the y axis represents the water level on the deck. The black rectangle shapes represent the hull which has bow flare angle of 90 degrees, the blue circles represent 75 degrees and the red triangles represent 60 degrees.

First, when the wave steepness is the largest 0.06, in the long wavelength range of 3m and 3.75m, the difference in water level on the deck was not significantly different even when the bow flare angle was applied. However, in the short wavelength of 2.25m, the water level decreased by 3% when the bow fare angle is 75 degrees and also decreased by about 8% when the bow flare angle is 60 degrees. Second, when the wave steepness is 0.05, the water level on the deck tends to decrease in the entire wavelength range. Particularly, in the wavelength of 3m, the water level on the deck decreases by about 19% when the bow flare angle is 75 degrees, and it also decrease by about 19% when it is 60 degrees. At other wavelengths of 2.25m and 3.75m, the water level difference on the deck is within 10%. Finally, when the wave steepness is the smallest 0.04, the water level on the deck tends to decrease as well. When the bow flare angle was applied at 2.25m which is the shortest wavelength range, the difference of the water level on the deck was within 3%. However, at the wavelength of 3m, it was decreased by about 12% when the bow flare angles were both 75 and 60 degrees. Finally, at the longest wavelength range of 3.75m, it was decreased by 2% at 75 degrees which does not show a big difference. But it decreased by 8% at 60 degrees. This is because when the bow flare angle is 60 degrees the amount of the water coming from the sides of the deck is smaller than when the bow flare angle is 75 degrees. However, the effect of the bow flare angle seems to be small when the wavelength is short, and effect of the bow flare angle is large when the wavelength is large.

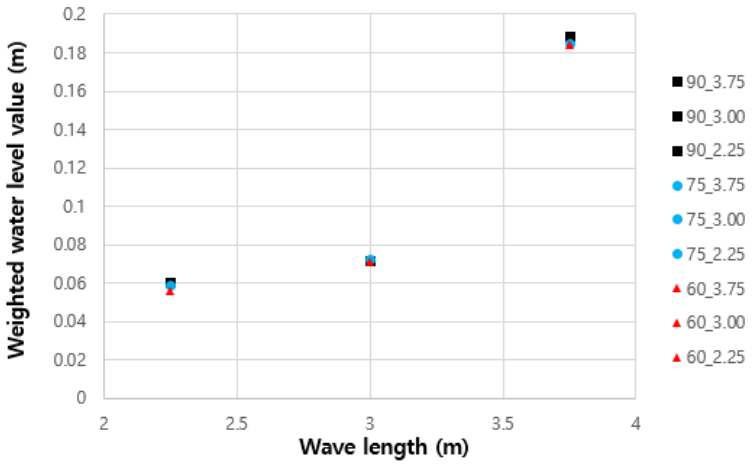

Figure 36 Comparison of the weighted water level on the deck value for FPSO models when the wave steepness is 0.06

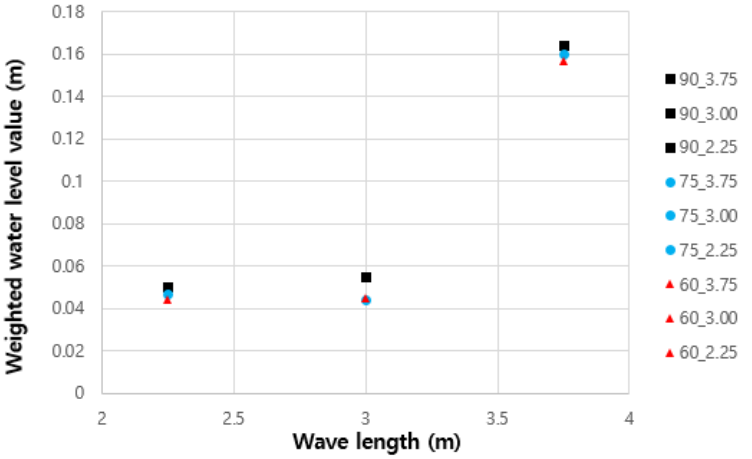

Figure 37 Comparison of the weighted water level on the deck value for FPSO models when the wave steepness is 0.05

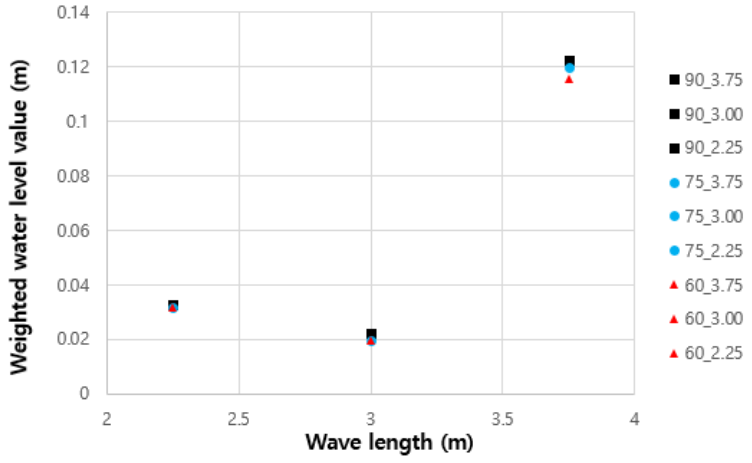

Figure 38 Comparison of the weighted water level on the deck value for FPSO models when the wave steepness is 0.04

6.2.3 Velocity on deck

In this study, water velocity was also measured on the deck when the green water occurred. Generally, the water velocity is measured at the center of the deck because the largest velocity occurs in the x direction, which is the longitudinal direction of the ship, on the center line of the deck. The water velocity of the deck is also considered to be an important factor affecting the pressure of the superstructure and deck.

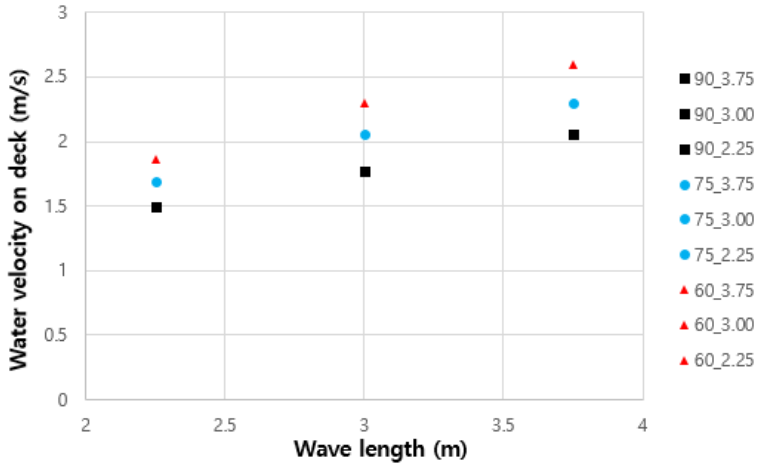

Figure 39 Comparison of the wave velocity on the deck for FPSO models when the wave steepness is 0.06

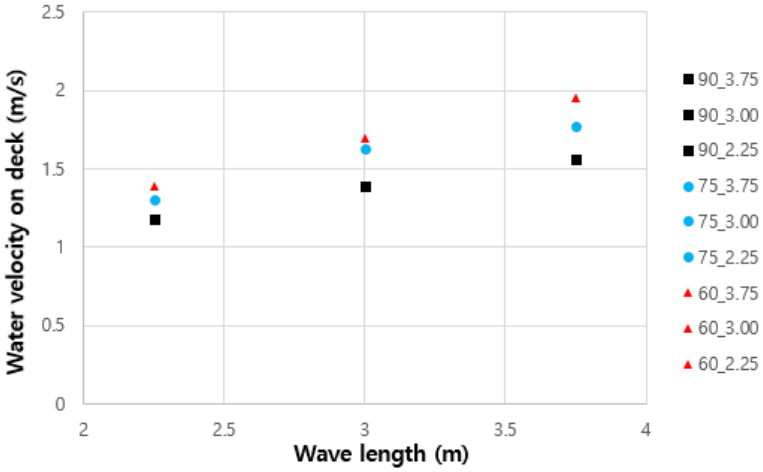

Figure 40 Comparison of the wave velocity on the deck for FPSO models when the wave steepness is 0.05

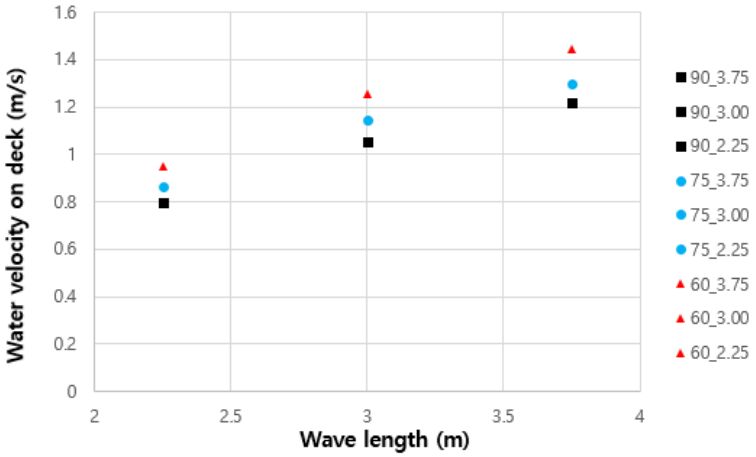

Figure 41 Comparison of the wave velocity on the deck for FPSO models when the wave steepness is 0.04

Figures 39 through 41 above show the water velocity on the deck relative to the wavelength for each wave steepness. The x axis of the graph represents the wavelength and the y axis represents the velocity. The black rectangle shapes represent the hull which has bow flare angle of 90 degrees, the blue circles represent 75 degrees and the red triangles represent 60 degrees.

Regardless of the wave steepness and the wavelength, the graphs above show that the smaller the bow flare angle, the faster the water velocity. When the wave steepness was 0.06, the water velocity on the deck increased about 15% when the bow flare angle was 75 degrees and about 25% when the bow flare angle was 60 degrees. Especially at the longest wavelength of 3.75m, the water velocity on the deck increased about 30% when the bow flare angle was 60 degrees. And in the case of the other wave steepness, the water velocity on the deck was increased by about 10% when the bow flare angle was 75 degrees and by about 20% when the bow flare angle was 60 degrees. When the conventional ship which has bow flare angle of 90 degrees, it is judged that the water velocity in the x direction is decreased due to the superposition by the water coming from in front of the deck and water coming from the side of the deck. However, in the case of the hull with the bow flare angle, the amount of water coming from the side of the deck decreases, but the amount of incoming water from in front of the deck does not change, so the water velocity of the x directional on the deck tends to increase.

6.2.4 Pressure on deck

Figures 42 through 51 below show time series graphs of the pressure on the deck at each location during one period when the wave steepness is 0.04 and the wavelength and wave height are at their maximum values. The x axis represents physical time and y axis represents pressure at each location of the deck. The black solid line represents the hull which has bow flare angle of 90 degrees, the blue dash line represents 75 degrees and the red dash line represents 60 degrees.

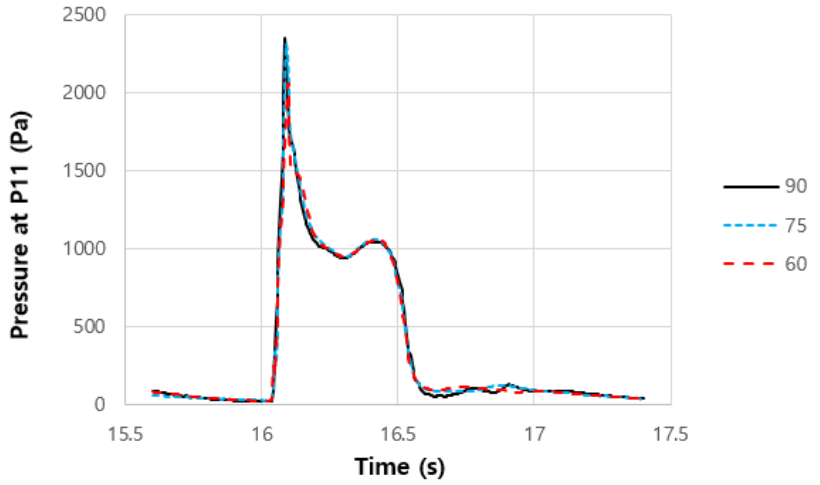

Figure 42 Comparison of the pressure time histories at P11 (S=0.04, λ =3.75, H=0.1500)

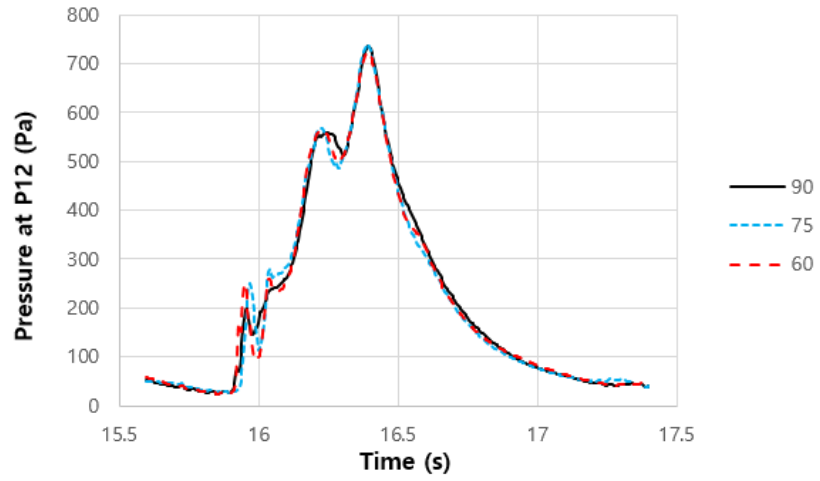

Figure 43 Comparison of the pressure time histories at P12 (S=0.04, λ =3.75, H=0.1500)

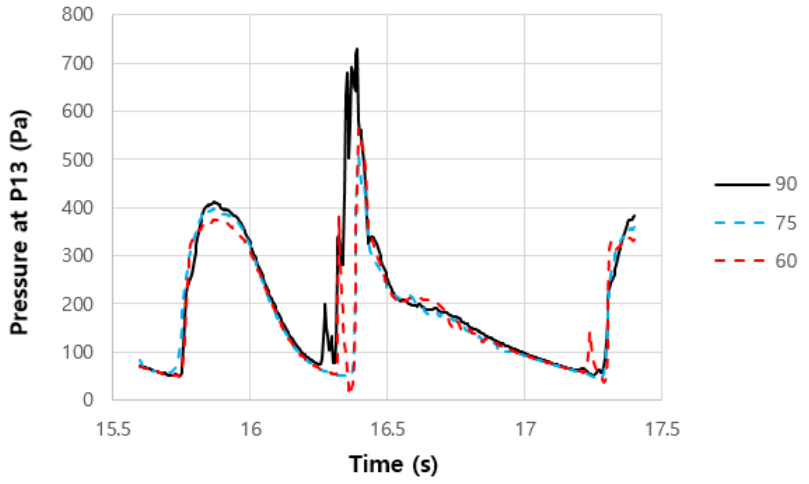

Figure 44 Comparison of the pressure time histories at P13 (S=0.04, λ =3.75, H=0.1500)

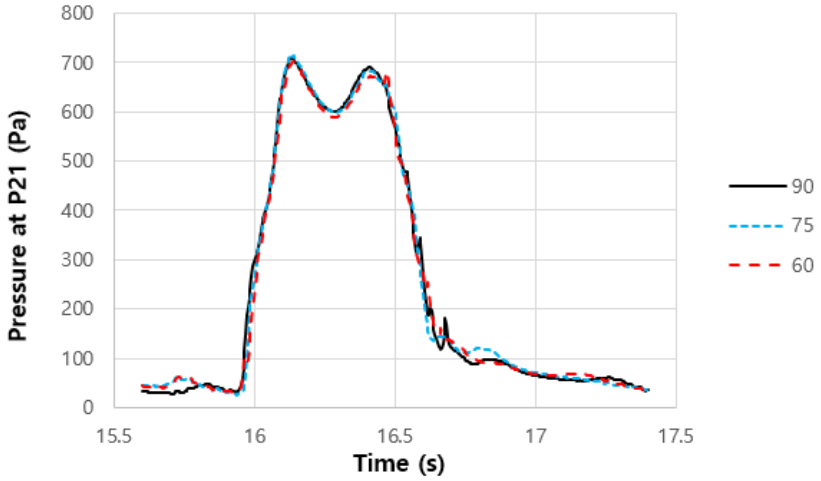

Figure 45 Comparison of the pressure time histories at P21 (S=0.04, λ =3.75, H=0.1500)

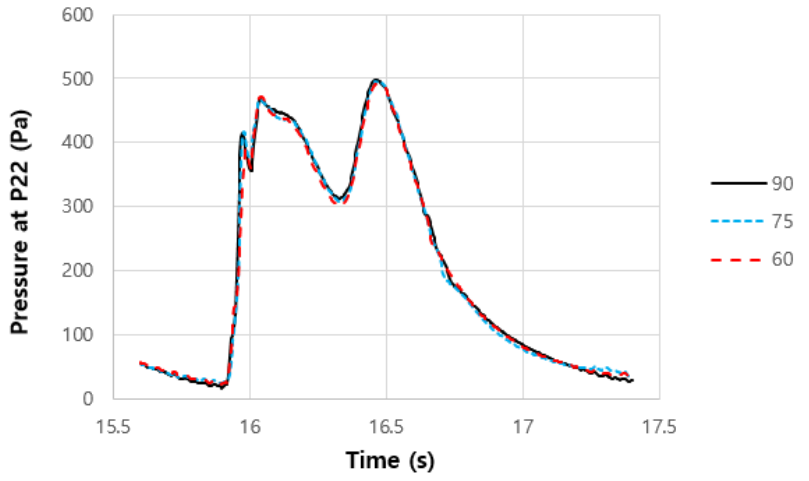

Figure 46 Comparison of the pressure time histories at P22 (S=0.04, λ =3.75, H=0.1500)

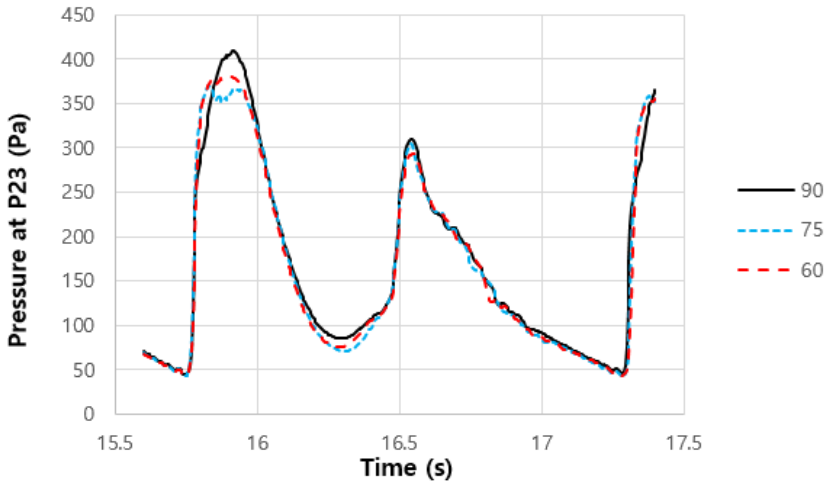

Figure 47 Comparison of the pressure time histories at P23 (S=0.04 λ =3.75, H=0.1500)

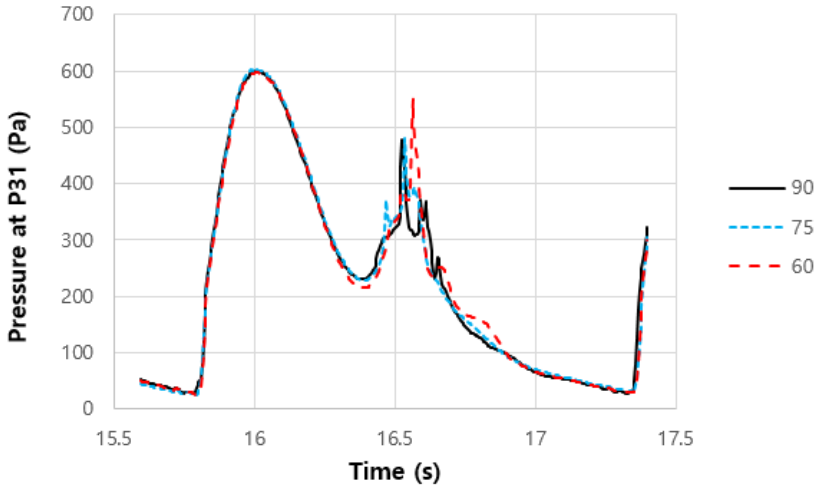

Figure 48 Comparison of the pressure time histories at P31 (S=0.04, λ =3.75, H=0.1500)

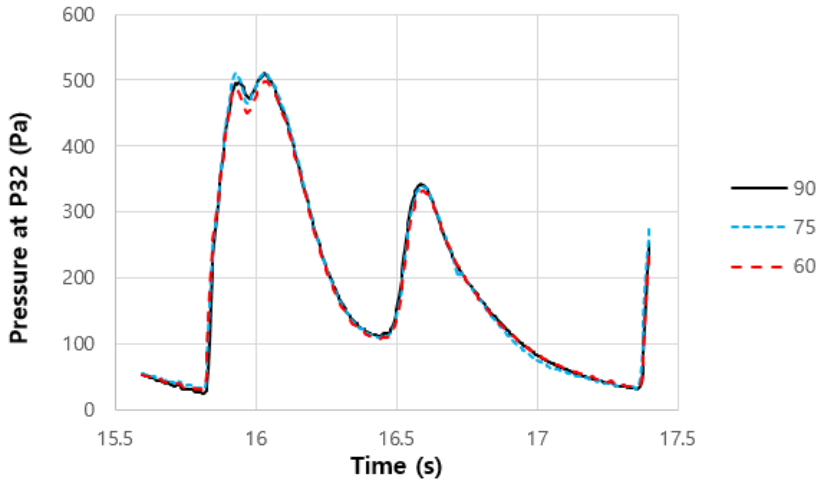

Figure 49 Comparison of the pressure time histories at P32 (S=0.04, λ =3.75, H=0.1500)

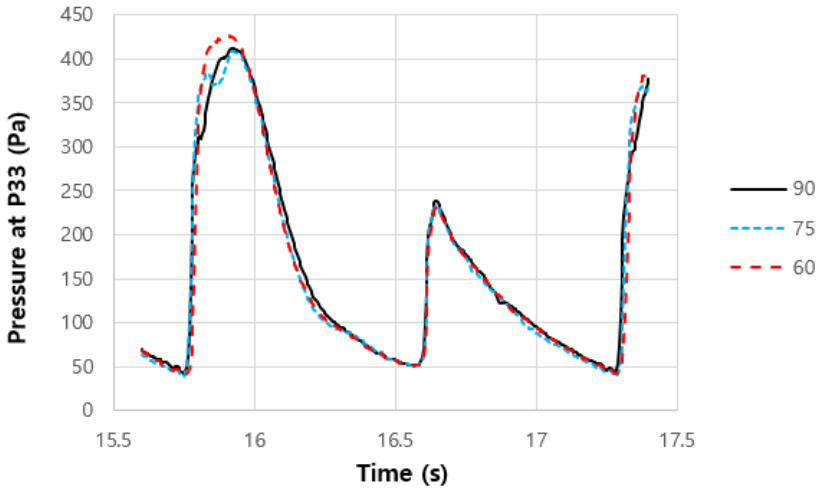

Figure 50 Comparison of the pressure time histories at P33 (S=0.04, λ =3.75, H=0.1500)

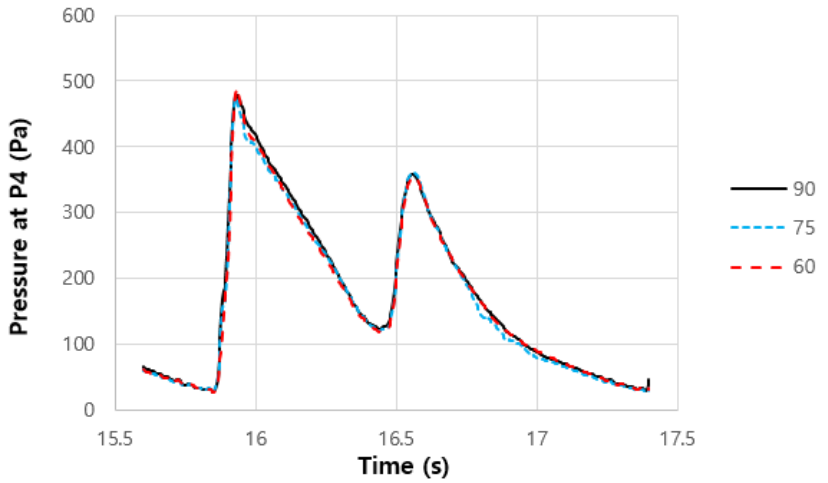

Figure 10 Comparison of the pressure time histories at P4 (S=0.04, λ =3.75, H=0.1500)

In the graphs at P13 and P23 which are located at side of the deck, when the bow flare angle is applied, the pressure on the deck tends to decreased when the initial water comes in. This is because the water level has decreased as mentioned before. However, the P31 and P32 at the front end of the deck seem to have little change in pressure. This is due to the fact that there is almost no change in the water level on the deck. Even though the water level has been reduced, there is almost no change in pressure at the P11 and P12 right in front of the superstructure as well. It is considered that the increasing water velocity in x direction at the center line of the deck affects the pressure

when the bow flare angle is applied. Therefore, it is considered that there is almost no change in the pressure at P11 and P12 due to the increase of the water velocity even though water level is decreased. At other locations, the bow flare angle seems to have little effect on pressure.

Figures 52 to 54 below show graphs of the pressure on the deck using weighted mean according to each wavelength in each wave steepness. The x axis of the graph represents the wavelength and the y axis represents weighted pressure value. The black rectangle shapes represent the hull which has bow flare angle of 90 degrees, the blue circles represent 75 degrees and the red triangles represent 60 degrees.

When the wave steepness is the largest 0.06, the pressure values decreased by about 3% when the wavelength was 2.25m and 3m even when the bow flare angle was applied. When the bow flare angle is applied even though the water level on the deck has decreased, it can be seen that there is almost no change in the pressure value in these two wavelength ranges. It also can be seen that the change of the pressure values is not large when the wave steepness is 0.04, 0.05 and the wavelength are 2.25m, 3m. However, at the longest wavelength of 3.75m and the wave steepness of 0.06, the pressure value decreased by 2% at 75 degrees, but increased by 7% at 60 degrees compared to the conventional ship which has bow flare angle of 90 degrees. When the wavelength is 3.75m and the bow flare angle is 60 degrees, even though the water level on the deck was decreased, the pressure value was increased due to the fact that the rate of increase in the water velocity on the deck is very large compared to other cases. However, when the wave steepness is 0.05 and 0.04, the effect of the bow flare angle is shown at a wavelength of 3.75m. When the bow flare angle is 75 degrees, there is almost no change in the pressure value, but when the bow flare angle is 60 degrees, it is decreased by about 8%. In the case of these two wave steepness, it is considered that the rate of decrease in the water level on the deck has a greater influence on the pressure value than the rate of increase in the water velocity on the deck.

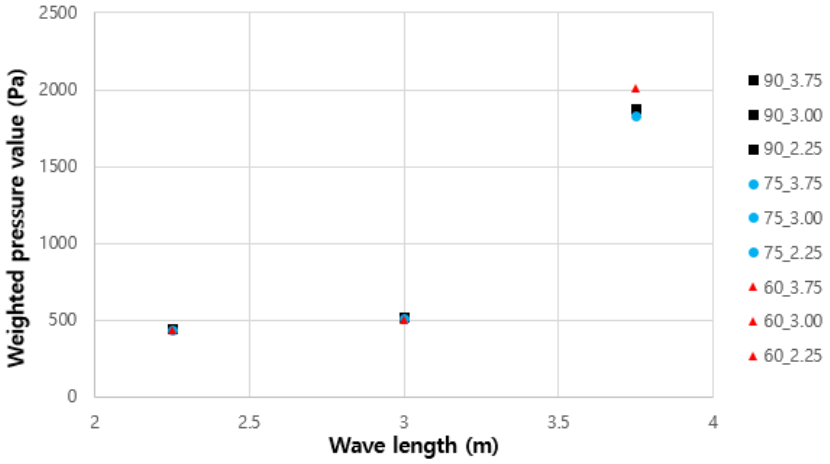

Figure 52 Comparison of the weighted pressure value for FPSO models when the wave steepness is 0.06

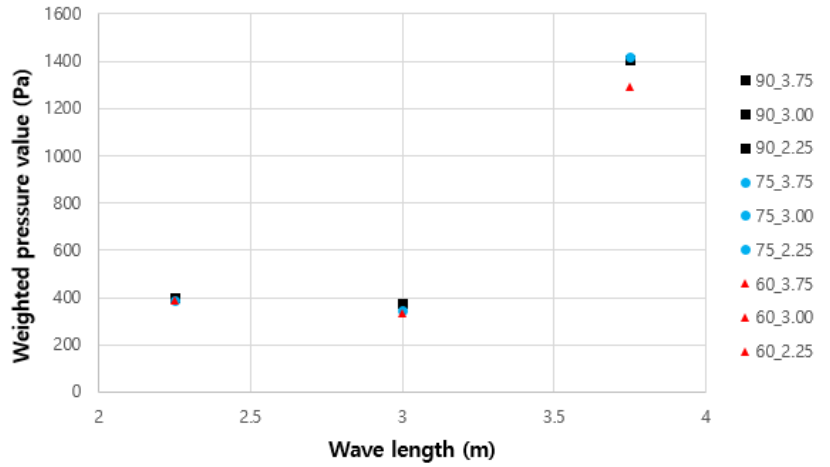

Figure 53 Comparison of the weighted pressure value for FPSO models when the wave steepness is 0.05

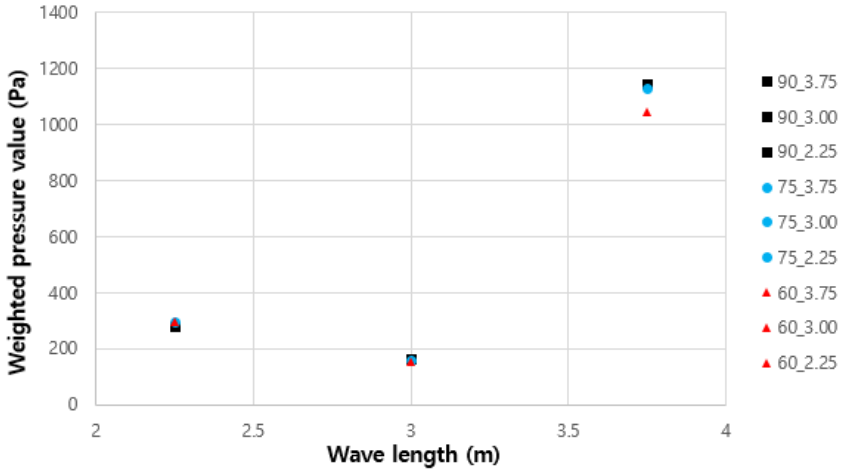

Figure 54 Comparison of the weighted pressure value for FPSO models when the wave steepness is 0.04

6.2.5 Force on superstructure

Finally, in this section, the force on the superstructure will be compared when the bow flare angle is applied. Figures 55 to 57 below show the force on superstructure relative to the wavelength for each wave steepness. The x axis of the graph represents the wavelength and the y axis represents the force. The black rectangle shapes represent the hull which has bow flare angle of 90 degrees, the blue circles represent 75 degrees and the red triangles represent 60 degrees.

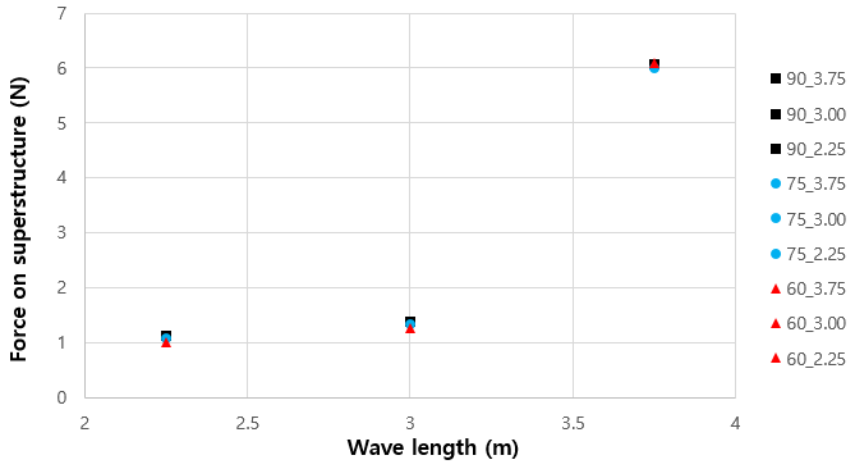

Figure 55 Comparison of the force on superstructure for FPSO models when the wave steepness is 0.06

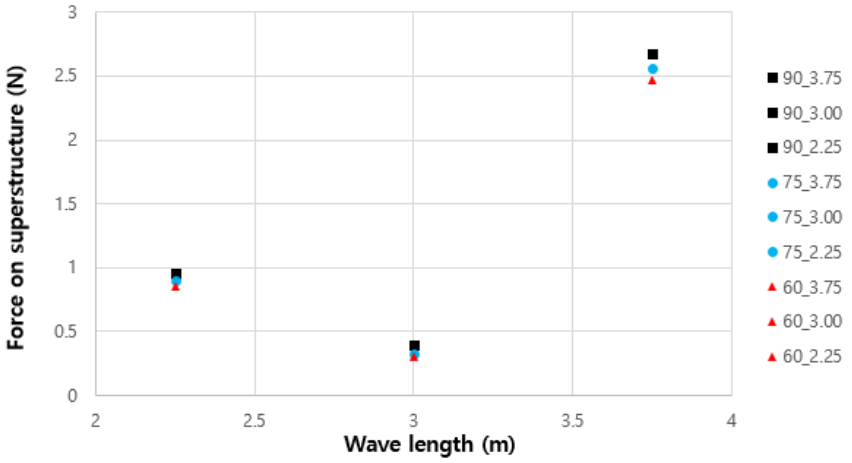

Figure 56 Comparison of the force on superstructure for FPSO models when the wave steepness is 0.05

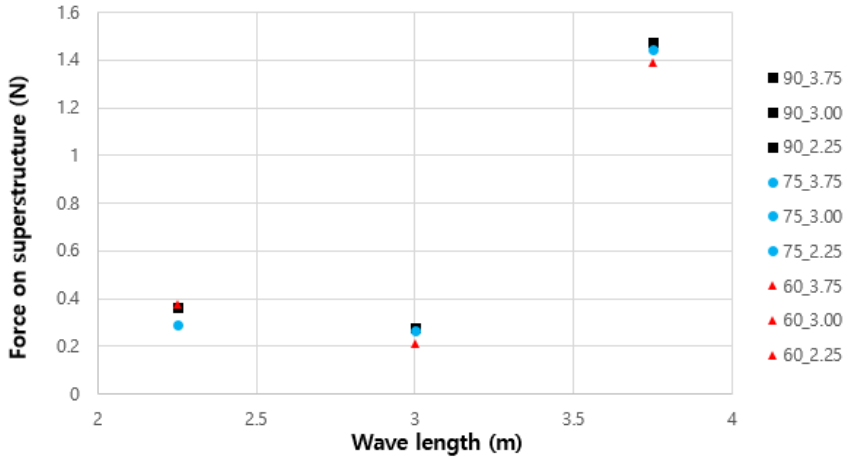

Figure 57 Comparison of the force on superstructure for FPSO models when the wave steepness is 0.04

First, when the wave steepness is 0.06, it can be seen that the force on superstructure is decreased due to the effect of the flare angle when the wavelength is 2.25m and 3m. But at the wavelength of 3.75m, even though the water level on the deck decreased, the pressure increased as the water velocity increased. Therefore, it can be confirmed that the force on superstructure when the green water occurs is not effective even when the flare angle is applied. However, when the wave steepness is 0.05 and 0.04, it can be confirmed that the force on superstructure is reduced in the entire wavelength range when the bow flare angle is applied. When the bow flare angle was 75 degrees, the maximum reduction rate was shown when the wave steepness was 0.04 and wavelength was 2.25m, and the force on superstructure decreased by about 15%. However, in other ranges, it showed a decreased rate of less than 5%. And when the bow flare was 60 degrees, in the 3m wavelength, the force on superstructure was reduced by about 20%, which represents the biggest decrease rate. And in the largest wavelength 3.75m, the force on superstructure was reduced by about 7%.

In summary, the above results show that even if the bow flare angle is applied, the effect of the bow flare angle is not observed when the wave steepness is large, but it is effective when the wave steepness is smaller than 0.06. This is because the bow flare angle reduces the amount of water coming from the side of the deck and reduces the force on superstructure. But when the wave steepness is 0.06, since the rate of increase

of the water velocity is large, it is considered that there is little change in the force on superstructure even though the water level on the deck is decreased.

7 Conclusions and discussions

In this study, the effect of the bow flare angle on the green water loading on the deck was investigated in order to present the appropriate bow flare angle. CFD was used to calculate the FPSO models with three different bow flare angles in regular head waves. The following conclusions can be drawn from the results of some limitations such as inflow wave, ship motions, and bow shape and so on.

1) In this study, when the flare angle is applied, it is confirmed that the wave height near the side of the deck is lowered when the green water occurs. Thereby reducing the amount of water coming in from the side of the deck. Also, the smaller the bow flare angle, the less amount of the water comes in from the side of the deck.

2) As the bow flare angle decreases, the water velocity on the deck tends to increase. Also, as the wave steepness increase, the rate of increase also increases. This is because when the green water occurs, the incoming water from the front of the deck and the incoming water from the side of the deck are combined. But, when the bow flare angle is applied, the amount of the incoming water from the side of the deck is decreased. Although the water coming from the front of the deck is constant regardless of the bow flare angle, the constant water velocity in the x direction is maintained. But the amount of the water coming from the side of the deck decrease, so that the velocity is increased.

3) When the bow flare angle was applied, the pressure on the deck decreased because the water coming in from the side of the deck reduced. But when the wave steepness is 0.06 and the wavelength is the largest 3.75m, even though the water level on the deck decreases, the pressure value increases due to the fact that the water velocity on the deck increases. This is because the effect of the increase in velocity is larger than the effect on pressure due to the reduction in the water level on the deck. But when the wave steepness is lower than 0.06,

as the rate of increase of the water velocity is small, the pressure value decrease because of the decrease in the water level on the deck.

4) When the wave steepness is 0.06 and the wavelength is 3.75m, as the pressure on the deck increase, the force on superstructure also slightly increased. However, when the wave steepness is lower than 0.06, the force on superstructure decreased over the entire wavelength range. The smaller the wave steepness, the larger the reduction of the force on superstructure. This is because the rate of decrease in the water level on the deck is similar regardless of the wave steepness, but the force on superstructure is further reduced when the wave steepness is 0.04, because the rate of the increase of the water velocity is smaller than other wave steepness.

5) In this study, when the bow flare angle was designed, only the front part of the bow that meets the incident wave was changed. But if the flare angle is also applied to the side of the deck, it can affect the amount of water entering the deck, and the pressure can be further reduced.

6) In order to focus on the deck pressure, water level on the deck and flow propagation process by only the green water, in this study the ship motions did not considered. But when the green water occurs, relative motion between the incident wave and the ship motions are also important parameter. So, afterward, considering the ship motions will also allow to study the effect of the bow flare angle in more detail. And, also very simplified model was selected in this study. So, afterward, considering the real FPSO model will be studied the effect of the bow flare angle.

7) This study shows some difference when the wave steepness is small when compared with the pressure data of SNU experimental data. In numerical calculation, the pressure value is greatly affected by the time step size and the size of the surface grid on the deck, and the size of the grid around the object. Therefore, in order to show better results in comparison with the experimental

results in the future, we will get more reliable results if we study the time step, gird size and so on.

References

Buchner, B., 2002. *Green Water on Ship-Type Offshore Structures*. Ph. D thesis, Delft University of Technology, The Netherlands.

Barcellona, M. Landrini, M. Greco, M. & Faltinsen, O.M., 2003. An Experimental Investigation on Bow Water Shipping. Journal of Ship Research, 47(4), pp.327-346.

Dallinga, R.P. & Gaillarde, G., 2001. Hatch Cover Loads Experienced by M.V. Derbyshire during Typhoon Orchid, International Workshop on Safety of Bulkcarriesrs, Glasgow.

Ersdal, G. & Kvitrud, A., 2000. Green water incident on Norwegian Production Ships. 10th International Society of Offshore and Polar Engineering Conference, Seattle, United States of America, 1, pp.211-218.

Yoon-Jin Ha., 2012. An Experimental Study on the Effects of Bow Flare Angle about Green Water in Regular Waves. Journal of the Society of Naval Architects of Korea, Vol. 49, No. 1, pp. 79-86.

Buchner, B and Arjan Voogt., 2000. THE EFFECT OF BOW FLARE ANGLE ON FPSO GREEN WATER LOADING. Proceeding of ETCE/OMAE2000 Joint Conference Energy for the New Millenium, New Orleans, LA

Hyun-Ho Lee., 2012. Experimental investigation of green water on deck for a CFD validation database. Ocean Engineering 42, 47-60.

Cezar Augusto Bellezi., 2013. A Numerical Study of the Effects of Bow Shape on Green Water Phenomenon. Proceedings of the Twenty-third International Society Offshore and Polar Engineering (ISOPE), USA.

Buchner, B., 2003. DESIGN ASPECTS OF GREEN WATER LOADING ON FPSOs. The 22nd International Conference on Offshore Mechanics & Arctic Engineering, Cancun, Mexico.

Yong Jig Kim., 2017. Computation of the Green Water Design Impact Loads Acting on the Box-Type Structure of a High-Speed Ship's Bow. Journal of the Society of Naval Architects of Korea, Vol. 54, No. 1, pp. 34-42.

Faulkner, D., 2001. Survival Design of Cargo Hatch Structures. RINA Conference Design and Operation for Abnormal Conditions II, London, United Kingdom.

Faltisen, O.M. Greco, M. & Landrini, M., 2002. Green Water Loading on FPSO. Journal of Offshore Mechanics and Arctic Engineering.

Greco, M. Faltinsen, O.M. & Landrini, M., 2005. Shipping of Water on A Two-dimensional Structure. Journal of Fluid Mechanics, 525, pp.309-332.

Jeong, K.L. Lee, Y.G. & Kim, N.C., 2009. A Fundamental Study for the Numerical Simulation Method of Green Water Occurrence on Bow Deck. Journal of the Society of Naval Architects of Korea, 47(2), pp. 188-195.

Leonhardsen, R.L. Ersdal, G. & Kvitrud, A., 2001. Experience and Risk Assessment of FPSOs in Use on the Norwegian Continental Shelf: Descriptions of Events. 11th International Society of Offshore and Polar Engineering Conference, Stavanger, Norway, 1, pp. 309-314.

Lloyd, A.J.R.M. Salsich, J.O. & Zseleczky, J.J., 1985. The Effect of Bow Shape on Deck Wetness in Head Seas, RINA.

O'Dea, J.F. & Walden, DA., 1984. The Effect of Bow Shape and Nonlinearities on the Prediction of Large Amplitude Motion and Deck Wetness. 15th Symposium On Naval Hydrodynamics, Hamburg, National Academy Press, Washington D.C., pp. 163-176.

Shin, K.S., 2005. Numerical Calculation and Experiment of Green Water on the Bow Deck in Regular Waves. Journal of the Society of Naval Architects of Korea, 42(4), pp. 350-356.

Ogawa, Y., 2003. Long-term prediction method for the green water load and volume for an assessment of the load line. J. Mar. Sci. Technol. 7, 137-144.

Seo, J.H., Seol, D.M., Lee, J.H., Rhee, S.H., 2010. Flexible CFD meshing strategy for prediction of ship resistance and propulsion performance. Int. J. Naval Arch. Ocean Eng. 2 (3), 139-145.

Sgouros, G.E., Pritchett, W.M., Schafer, D.R., Jones, D.L., 2005. Shell's experience with hurricane Ivan. In: Proceedings of API-2005 Hurricane Readiness and Recovery Conference, Houston, USA

Soares, C.G., Pascoal, A, 2005. Experimental study of the probability distributions of green water on the bow of floating production platforms. J. Offshore Mech. Arct. Eng. 127, 234-242.

Wang, G., Spong, R., 2003. Experience based data for FPSO's structural design. In: Proceedings of Offshore Technology Conference, Houston, USA, OTC 15068.

Drake, K.R., 2000. Transient Design Waves for Green Water Loading on Bulk Carriers, Transactions of RINA, Part C, pp 217-229.

Meskers, G., 2002. Realistic Inflow Conditions for Numerical Simulation of Green Water Loading, Master's thesis, Delft University of Technology/MARIN.

Mizoguchi, S., 1988. Analysis of Shipping Water with the Experiments and the Numerical Calculations, JSNA, Japan, Volume 163.

Mizoguchi, S., 1989, Design of Freeboard Height with the Numerical Simulation on the Shipping Water, PRADS'89.

Morris, W.D.M., Millar, J. and Buchner, B., 2000, Green Water Susceptibility of North Sea FPSO/FSUs, 15th Conference on Floating Production Systems (FPS), London.